Resonant photon scattering from ^{206,207,208}Pb and ^{209}Bi

T. Chapuran,* R. Vodhanel, and M. K. Brussel
Department of Physics, University of Illinois at Urbana-Champaign, Urbana, Illinois 61801
(Received 24 March 1980)

Resonant photon scattering from ^{206,207,208}Pb and ^{209}Bi has been measured from 4 MeV to the neutron thresholds using enriched targets, Ge(Li) detectors and bremsstrahlung beams with end-point energies of 7.0, 7.5, 7.6, 8.0, 8.5, and 10.4 MeV. Energies and values of $g\Gamma_0{}^2/\Gamma$ were obtained for many levels not observed in previous photon experiments. Spins of levels in ^{206}Pb and ^{208}Pb were determined from the angular distributions, and ground-state branching ratios were obtained from self-absorption measurements for seven transitions in ^{208}Pb. The results are compared with earlier spectroscopic studies and with lower resolution average cross-section measurements. The spectra of ^{207}Pb and ^{209}Bi are discussed in terms of the excitations of the ^{208}Pb core.

[NUCLEAR REACTIONS ^{206,207,208}Pb, ^{209}Bi(γ,γ); enriched targets; resonance fluorescence with 7.0, 7.5, 7.6, 8.0, 8.5, and 10.4 MeV bremsstrahlung. Measured E_γ, I_γ at 90° and 127°, and self-absorption; deduced $g\Gamma_0{}^2/\Gamma$, Γ_0/Γ, J.]

I. INTRODUCTION

Photonuclear reactions have long been important for spectroscopic studies of low-lying nuclear states and for measurements of the properties of the giant dipole resonance. However, experimental difficulties have limited their applicability to the study of states lying below the giant dipole. This region contains important nuclear structure information. By way of illustration, it is well known that the elastic scattering of photons is dominated in heavy nuclei by electric dipole excitations. The distribution of $E1$ strength, and the strength and location of the giant resonance are both explained microscopically by the mixing of the shell model particle-hole states. Particularly interesting in this regard is the lead region. Because of its stable configuration, ^{208}Pb, which itself has been the subject of several such shell model calculations,[1-6] is considered as a core to which valence particles or holes may be added to describe neighboring nuclei.[7] As a result, the level structure of the neighbors is expected to be closely linked to that of ^{208}Pb, as is experimentally observed at low excitation energies.

Until recently, studies of photon scattering from bound states above 5 MeV have been hindered by a lack of adequate photon sources and detectors. Many results have been obtained using photon beams produced in nuclear reactions (e.g., neutron capture[8]) but systematic studies have been difficult due to the discrete nature of these sources. Bremsstrahlung produced by electron beams provides a continuous spectrum of photon energies, but traditionally such beams have been of limited value, either because their energies were below 5 MeV, or because they were available only with low duty factors ($\lesssim$0.1%), severely limiting the average counting rates obtainable in high resolution detectors. Such difficulties were overcome at Illinois with our first superconducting electron accelerator[9] MUSL-1, whose beams of 40% duty cycle were used in nuclear resonance fluorescence measurements[10,11] to survey strong photon transitions in the regions of $A = 90$ and 208.

With the availability of our second generation accelerator[12] MUSL-2, we were able to make a more detailed and systematic study of the resonant photon scattering above 5 MeV from nuclei in the lead region. We built on the earlier work while incorporating major experimental improvements: use of a 100% duty factor beam of improved optical characteristics, an electronics system capable of handling higher instantaneous counting rates with better energy resolution, and expanded computer facilities for improved monitoring of experimental conditions and the acquisition of more extensive spectra. In addition we have more extensively utilized the continuous energy variability of the new accelerator to maximize our experimental sensitivity to weak and unresolved peaks, and to remove ambiguities due to branching. These changes led to a significant improvement in the accuracy and sensitivity of our measurements.

This paper presents the results of resonance fluorescence measurements on bound states in ^{206,207,208}Pb and ^{209}Bi. After reviewing the basic formulas in Sec. II and the experimental procedure in Sec. III, we present our data on the energies, decay widths, spins, and branching ratios of levels in these four nuclei. A comparison with earlier experimental and theoretical results is made, and the spectra of ^{207}Pb and ^{209}Bi are discussed in terms of the excitations of the ^{208}Pb core.

II. BASIC CONSIDERATIONS

Nuclear resonance fluorescence[13] (NRF) refers to the photoexcitation of a nucleus from its ground state (spin J_0) to an excited state (spin J_e) and the subsequent photon decay to the final state i. The cross section is given by

$$\sigma_{sc}^{i}(E)=\frac{\pi\lambda\!\!\!^{-2}}{2}\,g\,\frac{\Gamma_0\Gamma_i}{(E-E_r)^2+\Gamma^2/4}\ , \tag{1}$$

where E and $2\pi\lambda\!\!\!^{-}$ are the energy and wavelength of the incoming photon, Γ is the decay width of the resonant state at energy E_r, and Γ_i is the partial width for photon decay to the state i ($i=0$ denotes the ground state). g is the statistical factor $(2J_e+1)/(2J_0+1)$. The resonant photonuclear absorption cross section is related to the elastic scattering by

$$\sigma_{abs}(E)=\frac{\Gamma}{\Gamma_0}\,\sigma_{sc}^{0}(E)\,. \tag{2}$$

These formulas must be generalized[13] to account for the Doppler broadening due to thermal motions of the target nuclei:

$$\sigma_{\{\substack{sc\\abs}\},D}(E)=\sigma_{\{\substack{sc\\abs}\}}(E_r)\psi(x,t)\,. \tag{3}$$

ψ is an integral function[13] of $x=2(E-E_r)/\Gamma$ and $t=(\Delta/\Gamma)^2$, where the Doppler width Δ equals $E(2kT/Mc^2)^{1/2}$. At $E=7$ MeV and $T=300$ K, Δ is 16 eV for ^{11}B and 3.6 eV for ^{208}Pb. Although $\psi(x,t)$ has been derived assuming a Maxwellian velocity distribution, the effects of lattice binding in a solid target can be included[13-15] simply by use of a higher (effective) temperature in the formula for Δ.

Taking account of atomic and resonant nuclear absorption in the target, the number of elastically scattered photons detected at an angle θ relative to the beam axis is given by

$$N_{det}=N_{inc}(E_r)\epsilon(E_r)W(\theta)A'(g,\Gamma,\Gamma_0,\Delta/\Gamma)\,, \tag{4}$$

with

$$A'=n_s\int_{resonance}dE\,\sigma_{sc,D}^{0}(E)\,\frac{1-e^{-\alpha(E)}}{\alpha(E)}$$

and

$$\alpha(E)\equiv n_s\sigma_{abs,D}(E)+2\sum_j\eta_j\sigma_{at,j}(E)\,.$$

In formula (4), $N_{inc}(E)$ is the number of photons per unit energy incident on the target, $\epsilon(E)$ is the detection efficiency (including a solid angle factor $\Delta\Omega/4\pi$), and $W(\theta)$ is the angular distribution function for the emitted radiation. $\sigma_{at,j}$ represents the atomic absorption cross section for a particular element in the (symmetrically oriented) target, while $\eta_j(n_s)$ is the number of such atoms (or resonant scatterers) per unit area along the beam axis.

For a thin target $[\alpha(E_r)\ll 1]$ the analytical result $A'=n_s\pi^2\lambda\!\!\!^{-2}g\Gamma_0^{\,2}/\Gamma$ is independent of the Doppler width.[13] In our measurements the absorption effects were as large as 30%, and the A' integrals had to be evaluated numerically; nevertheless, their dependence on the nuclear parameters was largely unchanged from the thin target proportionality to $g\Gamma_0^{\,2}/\Gamma$. The determination of A' required knowledge of $N_{inc}(E_r)\epsilon(E_r)$. This product was in turn determined by observation of the scattering from levels whose nuclear parameters were known (see Sec. III).

In favorable cases, the excited state spin J_e (and therefore g) can be extracted from angular distribution measurements; additional information is required for the separate determination of Γ_0 and the branching ratio Γ_0/Γ. Since a direct observation of the inelastic scattering (and hence Γ_0/Γ) is difficult with a bremsstrahlung source, we have performed (in the case of ^{208}Pb) self-absorption measurements to provide an additional relationship between $g\Gamma_0$ and $g\Gamma_0^{\,2}/\Gamma$. Such measurements determine the effect on the scattering produced by a resonant absorber in the incident photon beam. The experimental result is expressed as a self-absorption ratio

$$R\equiv 1-C_{RA}/C_{NA}\,, \tag{5}$$

where $C_{RA}(C_{NA})$ is the counting rate for elastic scattering measured with a resonant (nonresonant) absorber in place. The use of a nonresonant absorber is important in that it eliminates effects not due to the resonant process. For a thin scatterer and a thin absorber (with n_a resonant nuclei per unit area) one finds

$$R\approx\frac{n_a\int\sigma_{abs,D}(E)\sigma_{sc,D}^{0}(E)dE}{\int\sigma_{sc,D}^{0}(E)dE}=2n_a\lambda\!\!\!^{-2}\frac{g\Gamma_0}{\Gamma}\int\psi^2(x,t)dx\,. \tag{6}$$

The integral involving the Doppler function ψ introduces an important dependence on Δ/Γ even in the thin target limit. If Doppler broadening can be neglected ($\Delta/\Gamma\ll 1$), the integral yields a constant and the self-absorption measurement determines $g\Gamma_0/\Gamma$. In the opposite case of extreme Doppler broadening ($\Delta/\Gamma\gg 1$) the integral is proportional to Γ/Δ. Then, the measurement determines $g\Gamma_0/\Delta$.

In most practical self-absorption experiments the thin target approximations are not appropriate and R must be evaluated numerically. Nevertheless, for the absorbers and scatterer used in this experiment, the branching ratio was well determined by the measurement of R for levels with $\Delta/\Gamma\ll 1$. When this extreme condition was not satisfied, a combination of the absorption and scatter-

ing measurements provided restrictions on the possible values of Γ_0 and Γ.

In conclusion, the combination of the elastic scattering, self-absorption, and angular distribution measurements can, under appropriate circumstances, independently determine the nuclear level parameters g, Γ, and Γ_0. An additional polarization measurement (see e.g., Ref. 8) could determine the parity change associated with the transition as well.

III. EXPERIMENTAL PROCEDURE

The bremsstrahlung beams used in this experiment were produced by electrons from the University of Illinois accelerator[12] MUSL-2, shown in Fig. 1 along with the transport to the experimental area. The electron beam from a 3 MeV Van de Graaff can be repeatedly passed through a 6 m superconducting linear accelerator section. The simple one pass beam, with an energy continuously variable up to 14 MeV, a current of $\lesssim 20$ μA, and a macroscopic duty cycle of 100% was ideally suited for resonance fluorescence measurements. An energy-analysis system in the extraction line was adjusted to allow a momentum spread of about 0.5% in the transported beam. In the experimental area, the beam was focused on a bremsstrahlung converter consisting of a 75 mg/cm^2 gold foil followed by a 14.8 g/cm^2 carbon beam stop, all mounted inside an insulated Faraday cup. The ~2 mm diameter beam spot was centered inside a 4 mm hole in a quartz viewscreen attached to the gold foil. The beam direction was defined by its position at the converter and by the requirement that it pass through the center of a quadrupole doublet 3 m upstream. Due to multiple scattering of the electrons in the converter, the photon beam was produced in a cone of half angle ~6°, resulting in a width [full width at half maximum (FWHM)] of about 14.5 cm at the target position 70 cm downstream.

The experimental arrangement is shown in Fig. 2. Photons scattered by a 10 cm square target were observed with a 55 cm^3 Ge(Li) detector at 127° relative to the incident beam. For the self-absorption measurements absorbers were inserted directly after the Faraday cup. For the spin determinations, additional scattering data were taken with the detector at 90°. The detector shielding was lead and tungsten, faced with copper and iron to reduce photoneutron production in the shielding.[10,11] The target-in to target-out background ratio for photon energies above a few MeV was typically larger than 15:1 for a 2 g/cm^2 lead target and 4:1 for a 3 g/cm^2 aluminum target. The background rises sharply at low energies; since the total counting rate must be limited due to pileup effects, and since we were operating with surplus beam intensity, the scattered beam was hardened with an absorber of copper and lead.

Signals from the detector were accumulated in

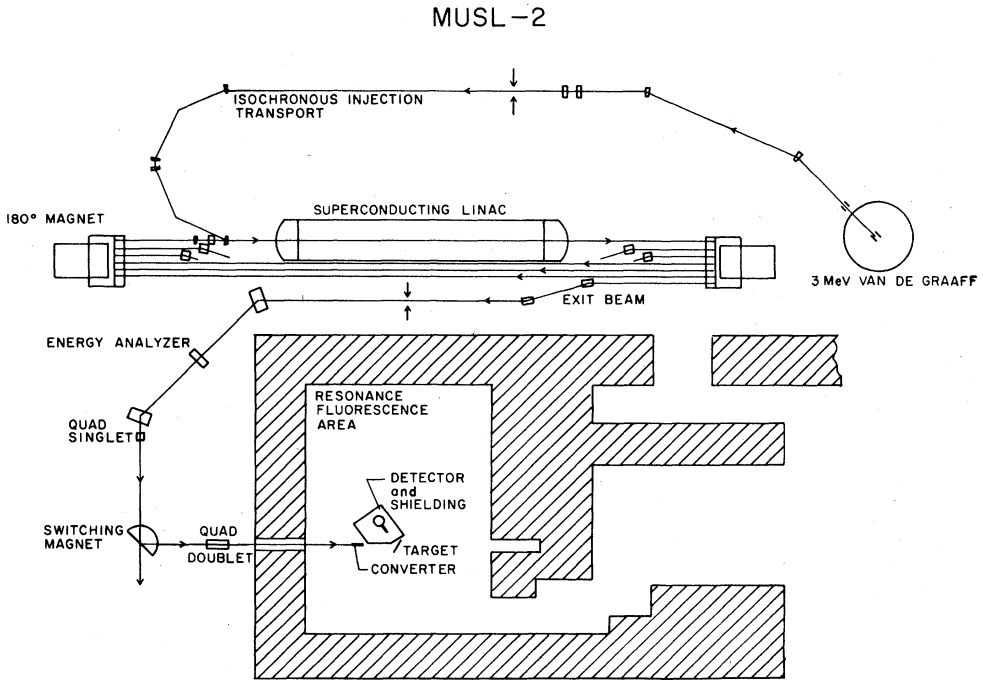

FIG. 1. MUSL-2 and the resonance fluorescence experimental area.

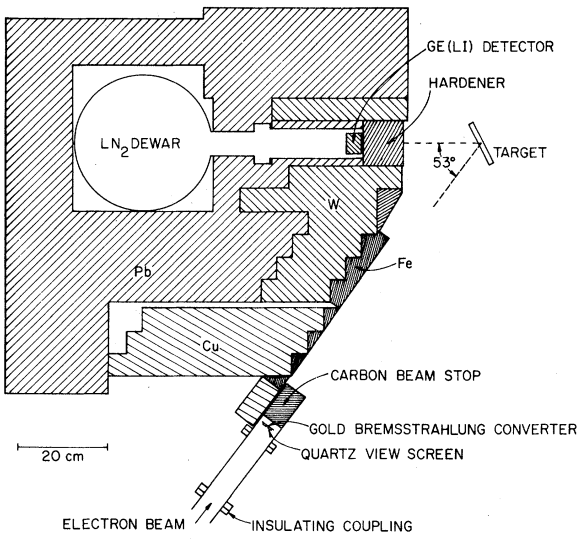

FIG. 2. Scattering geometry and shielding.

an 8192 channel spectrum in an on-line PDP-15 computer. Low energy events ($\lesssim$2 MeV) were rejected by a linear gate to minimize analog-to-digital converter (ADC) dead time, and a pileup rejection circuit maintained an acceptable energy resolution at high counting rates. Pileup losses and gain and zero shifts in the electronics were monitored with a precision, thermally stabilized pulser, triggered at a rate proportional to the beam intensity. The test pulses passed through the same linear chain as the photon pulses, but were identified and stored separately. Drift corrections calculated every five minutes from the positions of two pulser peaks were applied to the incoming data. The average counting rate in the detector was normally about 30 000 counts per second, resulting in pileup losses of about 40% of the total events. The resolution was typically 7 keV FWHM at 7 MeV for data accumulated over a two day run.

In the resulting spectra, full energy and escape peaks from the resonant scattering rest on a smooth background due to nonresonant scattering and Compton tails from higher energy photons. The peak centroids and areas were extracted from fits to the data with an empirical line shape and a smooth background, using the computer program[16] SAMPO.

The peak centroids were related to energies by a linear calibration based on levels excited in ^{11}B at 2.125, 4.445, 5.021, 7.286, and 8.920 MeV, using the known transition energies[17] (taking recoil into account) and the 511 keV spacing between the peaks in the Ge(Li) response function. Energies of strong levels were determined to within 1 to 2 keV.[18]

In the extraction of scattering cross sections from the peak areas [Eq. (4)], $N_{\rm inc}(E)\epsilon(E)$ was determined through an extensive calibration procedure[18] by measuring the scattering from nineteen levels in ^{11}B, ^{24}Mg, ^{27}Al, ^{31}P, ^{88}Sr, and ^{208}Pb (see Table I), whose nuclear parameters had been determined elsewhere.[17,19-32] An additional ten levels in ^{27}Al were also used as relative calibration points.[18] A complete calibration was performed for every 2 to 3 day run, with the electron charge collected in the Faraday cup serving as a relative monitor of the photon intensity. $N_{\rm inc}(E)\epsilon(E)$ was measured with seven different beam end-point energies from 7.0 to 11.3 MeV. For purposes of comparison, the hardener transmission and the efficiency function measured for a similar detector[33] were used to extract the incident photon intensity in each case. A composite of these results is shown in Fig. 3; a particular curve of 7.65 MeV end-point energy is displayed in Fig. 4. The data for each beam energy are well described by a simple exponential function over a large energy region (away from the endpoint). In these regions $N_{\rm inc}(E)\epsilon(E)$ was determined to within 15%.

The targets, scattering angles, and beam energies used in all of the experiments on lead and bismuth are summarized in Table II. Scattering measurements at 127° were made for all four nuclei. At this backward angle the atomic scattering background is reduced, while proximity to the zero of $P_2(\cos\theta)$ makes the angular distribution factor $W(\theta)$ identical for all dipole transitions (independent of J_0 and J_e). For the spin zero nuclei ^{206}Pb and ^{208}Pb, additional data were taken at 90°, the maximum of the quadrupole distribution. Dipole and quadrupole transitions were then easily distinguished on the basis of the relative yields at 90° and 127°. Finally, a self-absorption measurement was made for ^{208}Pb using an enriched scatterer, a resonant absorber of the same material, and a comparison absorber of ^{209}Bi of identical shape and thickness. The absorbers were interchanged every two hours to cancel the effects of any systematic changes in the resonant and nonresonant absorber spectra over the 24 h run. The counting rates and pileup losses were essentially the same in both spectra, and the peaks were fit with identical line shapes and similar backgrounds. A check for differences in the atomic absorption using a boron scatterer with the lead and bismuth absorbers showed no difference in the yields of the strong ^{11}B levels.

IV. RESULTS AND DISCUSSION

A. ^{208}Pb

The complete experimental results for ^{208}Pb are summarized in Table III. Values of $g\Gamma_0^2/\Gamma$ for 14

TABLE I. Level parameters used in $N_{inc}(E)\epsilon(E)$ calibration.

Nucleus	J_0^π	Energy (MeV)	J_e^π	Γ_0 (eV)	Γ_0/Γ	References
^{11}B	$\frac{3}{2}^-$	2.125	$\frac{1}{2}^-$	0.136 ± 0.010	1.0	17
		4.445	$\frac{5}{2}^-$	0.61 ± 0.03	1.0	17
		5.021	$\frac{3}{2}^-$	1.85 ± 0.18	0.83 ± 0.05	19–21
		8.920	$\frac{5}{2}^-$	4.55 ± 0.46	0.95 ± 0.01	17,20–22
^{24}Mg	0^+	9.827	1^+	1.05 ± 0.26	0.82 ± 0.08	23,24
				$1.7^{+1.0}_{-0.7}$		25
		9.965	1^+	4.50 ± 0.73	0.71 ± 0.06	23,24
				$6.2^{+2.7}_{-2.2}$		25
		10.711	1^+	16.6 ± 1.9	0.81 ± 0.04	24,25
^{27}Al	$\frac{5}{2}^+$	2.981	$\frac{3}{2}^+$	0.11 ± 0.01	1.0	24
^{31}P	$\frac{1}{2}^+$	3.134	$\frac{1}{2}^+$	0.062 ± 0.004	0.974 ± 0.003	24,26
		3.506	$\frac{3}{2}^+$	0.032 ± 0.005	0.62 ± 0.04	24
		7.139	$\frac{1}{2}^+$	1.45 ± 0.11	1.0	26–28
		8.209	$\frac{3}{2}^+$	1.4 ± 0.1	0.54	29
^{88}Sr	0^+	6.212	1	2.33 ± 0.22	1.0	30
		6.333	1	3.60 ± 0.35	1.0	30
^{208}Pb	0^+	4.842	1	6.9 ± 1.4	1.0	31
				5.1 ± 0.8		32
		5.293	1^-	7.0 ± 1.4	1.0	31
		5.512	1^-	21.4 ± 2.2	1.0	31
		7.063	1^-	16.9 ± 3.1[a]	1.0	31
		7.083	1^-	9.0 ± 1.6[a]	1.0	31

[a] $\Gamma_0 = 25.9 \pm 2.1$ from Ref. 31 for the unresolved 7.063–7.083 MeV doublet; the relative strengths are taken from our measurements.

levels were extracted from scattering measurements at 127° using enriched ^{208}Pb targets and bremsstrahlung produced by 7.00, 7.53, and 10.37 MeV electrons. The spins of the seven strongest levels were determined from scattering measurements at 127° and 90° using a 7.65 MeV beam; branching ratios for these levels were also obtained from self-absorption measurements using an 8.00 MeV beam.

The 7.0 and 7.5 MeV spectra are shown in Fig. 5; the strong, well-known levels at 4.842, 5.293, 5.512, 6.720, 7.063, 7.083, and 7.332 MeV are easily seen. The weaker levels ($\Gamma_0^2/\Gamma \lesssim 3$ eV) at 6.263, 6.312, and 6.363 MeV rise more clearly above the background in the 7.0 MeV data, demonstrating the enhanced sensitivity near the bremsstrahlung end point. The overall sensitivity of these measurements is indicated by the observation of levels at 5.948 and 7.243 MeV ($\Gamma_0^2/\Gamma = 1.0$ and 1.7 eV, respectively) which had not been detected in previous photon scattering experiments. Other levels of this strength may have been missed, however, because of the complicated ^{206}Pb spectrum (due to the 26% target contaminant) seen emerging from the background. Knowledge of this spectrum was essential in properly distinguishing the ^{208}Pb and ^{206}Pb peaks. In particular, levels in ^{206}Pb at energies near 6.720, 7.063, and 7.083 MeV produced approximately 15%, 6%, and 4%, respectively, of the resonant scattering observed from the enriched ^{208}Pb target at those energies. These effects, which have not been previously reported, would be still larger for the natural lead targets used in several earlier ^{208}Pb experiments. Measurements using enriched targets of both isotopes were combined in determining their respective contributions.

Additional data taken at 90° and 127° with a 7.65 MeV beam were used to determine the spins of the strongest levels. Table IV shows the measured ratios of the cross sections at 90° to 127°; the predicted values for dipole and quadrupole

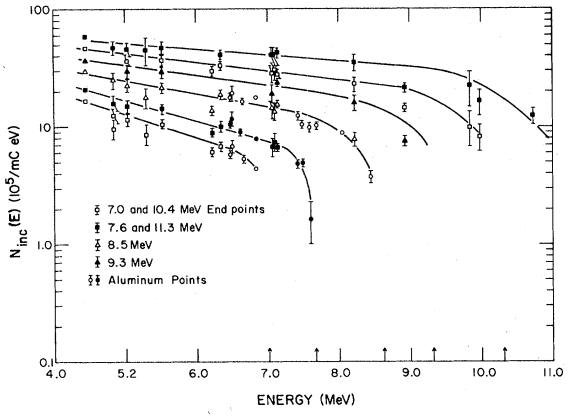

FIG. 3. Summary of photon intensity measurements for bremsstrahlung end-point energies of 7.00, 7.65, 8.50, 9.30, 10.37, and 11.32 MeV. $N_{inc}(E)$ is the number of photons per unit energy striking the target, per unit charge collected from the electron beam. The calibration levels listed in Table I are represented by squares and triangles; the ^{27}Al relative calibration lines (whose widths were measured with the 10.4 MeV beam) are represented by circles. The error bars include both statistical and calibration uncertainties. A few points at low energy or far from the curves are not included.

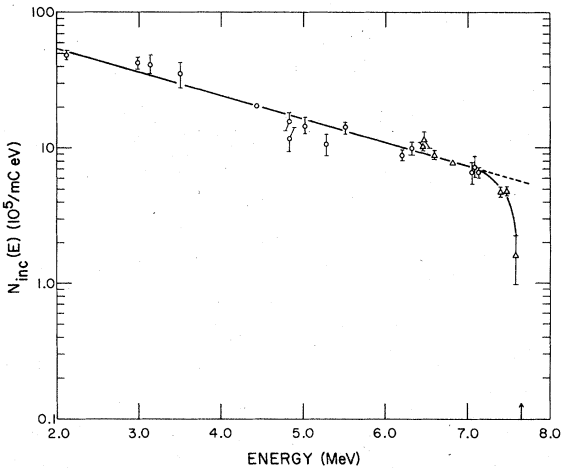

FIG. 4. Complete photon intensity measurement for the 7.65 MeV beam. Levels listed in Table I are represented by circles and the ^{27}Al relative calibration points by triangles. The error bars include both statistical and calibration uncertainties.

scattering are 0.73 and 2.20 (taking account of the finite angular acceptance). The listed uncertainties are statistical only; the measurement for the 4.085 MeV level has been included for completeness despite its poor statistics, since it is the only known quadrupole transition[34] that we observed.

The ratios for the remaining levels are in good agreement with the dipole prediction, consistent with earlier measurements of these spins.[34-37] The transitions at 5.948, 6.262, and 7.278 MeV were also reported to be dipole.[34,35,38] A dipole character for the remaining three excitations was assumed for the purpose of extracting the decay widths listed in Table III.

The uncertainties in the measured values of Γ_0^2/Γ listed in Table III include both statistical errors

TABLE II. Experiments performed on lead and bismuth isotopes.

Nucleus	$-Q(\gamma,n)$ (MeV)	Beam energy (MeV)	Scattering angle	Target thickness (g/cm^2)	Target isotopic abundances
^{206}Pb	8.1	8.50	127°	2.43	88.0% 206 9.0% 207 3.0% 208
		8.50[a]	90°	2.43	
^{207}Pb	6.7	7.00	127°	10.4avg[b]	2.6% 206 84.8% 207 12.6% 208
		7.65	127°	10.4avg[b]	
^{208}Pb	7.4	7.00	127°	2.14	25.8% 206 1.7% 207 72.5% 208
		7.53	127°	1.91	
		10.37[a]	127°	1.91	
		7.65	127°	3.54	
		7.65[a]	90°	3.54	
		8.00[c]	127°	2.14	
^{209}Bi	7.5	7.65	127°	3.11	100% 209

[a] Hardener was 62.5 g/cm^2 copper plus 21.6 g/cm^2 lead for these runs; for all other runs, 62.5 g/cm^2 copper plus 14.4 g/cm^2 lead were used.

[b] Open right circular cylinder: 5.4 cm outer diam × 4.7 cm inner diam × 5.5 cm. Mass = 309 g.

[c] Self-absorption experiment using 3.51 g/cm^2 enriched ^{208}Pb and 3.52 g/cm^2 ^{209}Bi absorbers.

TABLE III. ^{208}Pb results. The values for Γ_0^2/Γ have been extracted assuming $J=1$ where not measured (except $J=2$ for the level at 4.085 MeV). The listed uncertainties for Γ_0/Γ include statistical errors only, while those for Γ_0^2/Γ also include the uncertainty in $N_{inc}(E)\epsilon(E)$.

Energy (keV)	J	Γ_0^2/Γ (eV)	Γ_0/Γ
4085.2±2.0		0.68±0.15	
4841.6±1.0	1	5.0 ±0.8	$0.85^{+0.13}_{-0.09}$
5292.6±2.0	1	5.1 ±0.8	$0.78^{+0.22}_{-0.14}$
5512.2±1.0	1	22.3 ±3.4	$0.98^{+0.02}_{-0.04}$
5948.0±3.0		1.0 ±0.3	
6263.4±3.0		2.6 ±0.5	
6311.7±3.0		3.2 ±0.6	
6362.8±3.0		1.6 ±0.4	
6720.1±1.5	1	7.6 ±1.5	$1.00^{+0.00}_{-0.11}$
7063.3±1.5	1	15.7 ±2.6	$0.98^{+0.02}_{-0.07}$
7082.8±1.5	1	8.8 ±1.5	1.0[a]
7243.0±4.0		1.7 ±0.6	
7277.9±4.0		1.7 ±0.6	
7332.2±1.5	1	26.9 ±4.8	$1.00^{+0.00}_{-0.12}$

[a] See text for discussion.

and a 15% uncertainty in the value of $N_{inc}(E)\epsilon(E)$ for levels distant from the end-point energy. Widths of the levels at 7.063, 7.083, and 7.332 MeV are based on the 10.4 MeV data only, since the photon intensity at these energies was much less accurately determined with the 7.5 MeV beam. Where Γ_0/Γ was not measured, the listed widths were extracted from the scattering measurements assuming $\Gamma_0/\Gamma=1$. The value of $g\Gamma_0^2/\Gamma$ is nonetheless determined rather accurately in this way. For example, even for the very strong level at 5.512 MeV the assumption of a branching ratio of 0.5 would produce a value of $g\Gamma_0^2/\Gamma$ within 11% of that calculated for $\Gamma_0/\Gamma=1$.

Γ_0/Γ ratios for seven levels were extracted from the scattering and self-absorption measurements. For the latter the 2.1 g/cm^2 enriched ^{208}Pb scatterer was used with 3.5 g/cm^2 resonant and nonresonant absorbers. Figure 6 shows a portion of the spectrum obtained with each of the absorbers; the resonant absorption reduces the peak areas by about 40%. The results for the branching ratios in Table III are all consistent with nearly 100% decay to the ground state; the listed uncertainties are calculated from statistical errors only. We believe the total possible systematic error in the measurements to be less than a few percent, resulting in a possible 10% systematic error in the extracted branching ratios. Our measurement for the 7.083 MeV level corresponded to a branching ratio greater than unity (by almost two standard deviations). Systematic errors would all produce effects in the opposite direction. Since this anomaly appears to be statistical in nature, we have set $\Gamma_0/\Gamma=1$ for this level.

As an example, the combined results of the scattering and self-absorption experiments for the level at 4.842 MeV are displayed graphically in Fig. 7. Shown are the regions in the Γ_0 vs Γ plane consistent with each measurement, based on numerical calculations including absorption and Doppler broadening. The error band for the self-absorption measurement reflects statistical errors only, while that for the scattering also includes the $N_{inc}(E)\epsilon(E)$ uncertainty. The scattering curves lie near trajectories of constant Γ_0^2/Γ, with small deviations caused by absorption in the target. The self-absorption curves for large values of Γ approach straight lines drawn through the origin (trajectories of constant Γ_0/Γ), illustrating that the branching ratio is determined by the absorption measurement when Doppler broadening is negligible ($\Delta=2.5$ eV for this level). The shaded region in Fig. 7 is the locus of points consistent with both measurements which satisfy the additional requirement that $\Gamma_0/\Gamma\leq 1$. Corresponding results were obtained for the six other levels measured; several representative cases are shown in Fig. 8.

A comparison of our ^{208}Pb widths with those of other experiments is presented in Table V. Of the low resolution (~100 keV) photon scattering measurements, only the most recent, by Laszewski and Axel, are presented[31]; earlier studies were made by Reibel and Mann,[39] Fuller and Hayward,[40] and Axel *et al.*[41] The high resolution data were obtained from scattering and absorption measurements using photons produced by bremsstrahlung,[10,32,35,36] by (n,γ) reactions,[42,43] by the ^{19}F$(p,\alpha\gamma)^{16}$O reaction,[37,44,45] and by the ^{34}S$(p,\gamma)^{35}$Cl reaction.[46]

The first two columns of Table V show that the present results for the widths of the strong ^{208}Pb transitions are systematically smaller than those reported in an earlier version of this experiment by Coope *et al.*[10] This effect primarily results from changes in the $N_{inc}(E)\epsilon(E)$ calibration. The earlier calibration was based partly on preliminary tagged photon results[11,47] for ^{208}Pb and ^{88}Sr, which were systematically 15–20% higher than the values used here. Furthermore, because our measurements are more extensive (using more calibration levels and beam energies) a more accurate evaluation of the shape and magnitude of the $N_{inc}(E)\epsilon(E)$ curves was possible. This is reflected in the smaller uncertainties here assigned to widths of strong levels. On the other hand, our enhanced sensitivity to weaker levels is due to improved resolution and statistics, and to the continuously variable beam energy available with MUSL-2.

The comparison of our widths with recent reso-

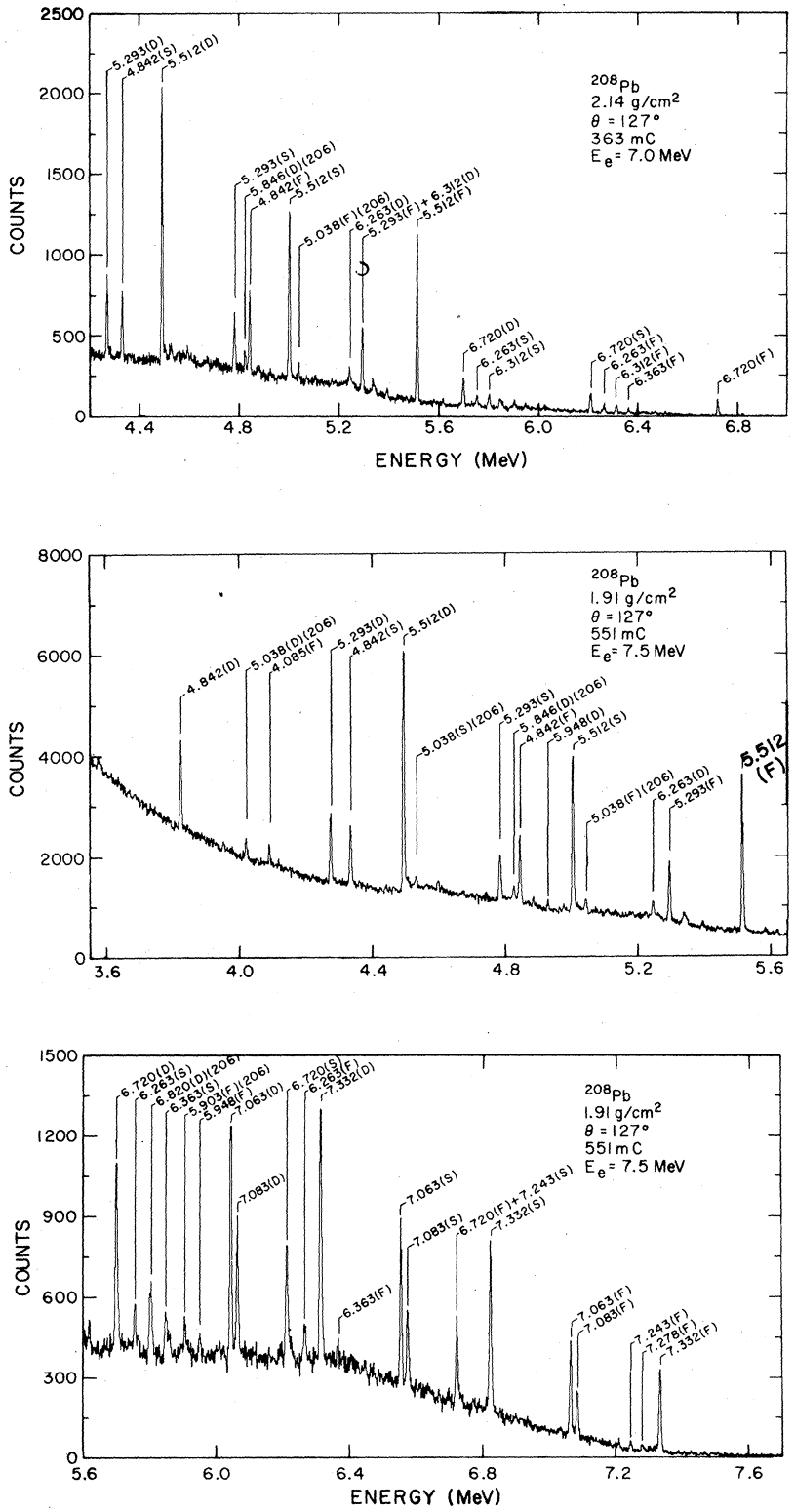

FIG. 5. Spectra for 7.0 MeV (upper figure) and 7.5 MeV (lower two figures) bremsstrahlung scattered from enriched (72.5%) ^{208}Pb targets. (*F*), (*S*), and (*D*) refer to the full energy, single-, and double-escape peaks, respectively. One channel corresponds to 1.36 keV in the 7.0 MeV spectrum, and 1.48 keV in the 7.5 MeV spectrum.

TABLE IV. ^{208}Pb angular distribution measurements. Listed uncertainties are statistical only.

Energy (MeV)	$W(90°)/W(127°)$	J
4.085	1.74±1.10	
4.842	0.71±0.07	1
5.293	0.74±0.12	1
5.512	0.68±0.04	1
6.720	0.71±0.07	1
7.063	0.76±0.05	1
7.083	0.72±0.08	1
7.332	0.75±0.09	1

	$W(\theta)$	$W(90°)/W(127°)$
Dipole	$1+0.500\,P_2(\cos\theta)$	0.73
Quadrupole	$1+0.357\,P_2(\cos\theta)+1.143\,P_4(\cos\theta)$	2.28[a]

[a] The experimental ratio for quadrupole scattering is reduced to 2.20 by the finite angular acceptance of the detector.

nance fluorescence measurements from Giessen[35] (shown in the third column of Table V) is reassuring. At Giessen, the shape of the incident photon spectrum was directly measured from the photodisintegration of deuterium. The absolute intensity was determined by the scattering from the 7.063 MeV level using the width reported by Coope *et al.*[10] For comparison with our data, we have renormalized their flux using the tagged photon result[31] for this level (with the relative strengths of the unresolved 7.063 and 7.083 MeV levels determined from the high resolution experiments). Such an adjustment yields widths and relative strengths for the remaining levels generally in good agreement with our own, and provides a check on our measurement of the shape of the incident photon spectrum.

The Illinois tagged photon measurements[31] listed in the fourth column of Table V represent the total photon strength contained within the ~100 keV resolution of the bremsstrahlung tagging process. The listed widths for the levels at 4.842, 5.293, 5.512, and 7.063–7.083 MeV (which are in reasonably good agreement with nearby calibration levels in other nuclei) have been used as part of the $N_{\rm inc}(E)\epsilon(E)$ calibration for the present experiment. However, near the 6.720 and 7.332 MeV transitions, the low resolution measurements indicate considerably more strength than was observed with the Ge(Li). This discrepancy may be due to the presence of additional weak levels in the vicinity of these two energies, levels too small to be individually seen above the background in our

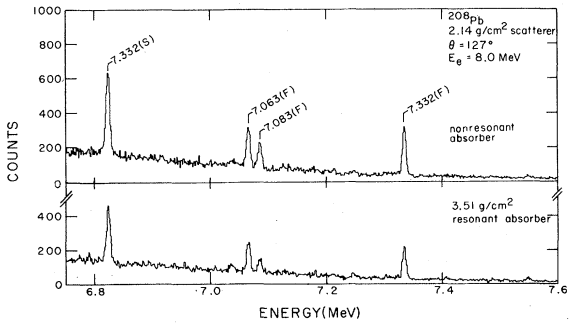

FIG. 6. Self-absorption experiment for ^{208}Pb. Shown is a portion of the spectrum obtained with the nonresonant (upper) and the resonant (lower) absorbers in place. The nonresonant spectrum has been normalized to account for the different integrated incident photon flux in the two runs. The peak areas are reduced in the lower spectrum due to the resonant absorption. One channel corresponds to 1.37 keV.

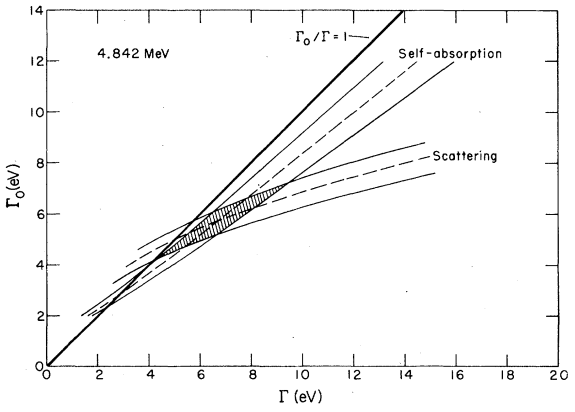

FIG. 7. Combined results of the self-absorption and scattering measurements for the 4.842 MeV level in ^{208}Pb. The dashed curves indicate combinations of Γ_0 and Γ which reproduce the experimental results; the solid curves represent the error band for each case. The shaded region contains the values of Γ_0 and Γ consistent with both experiments, and with the condition $\Gamma_0/\Gamma \leq 1$.

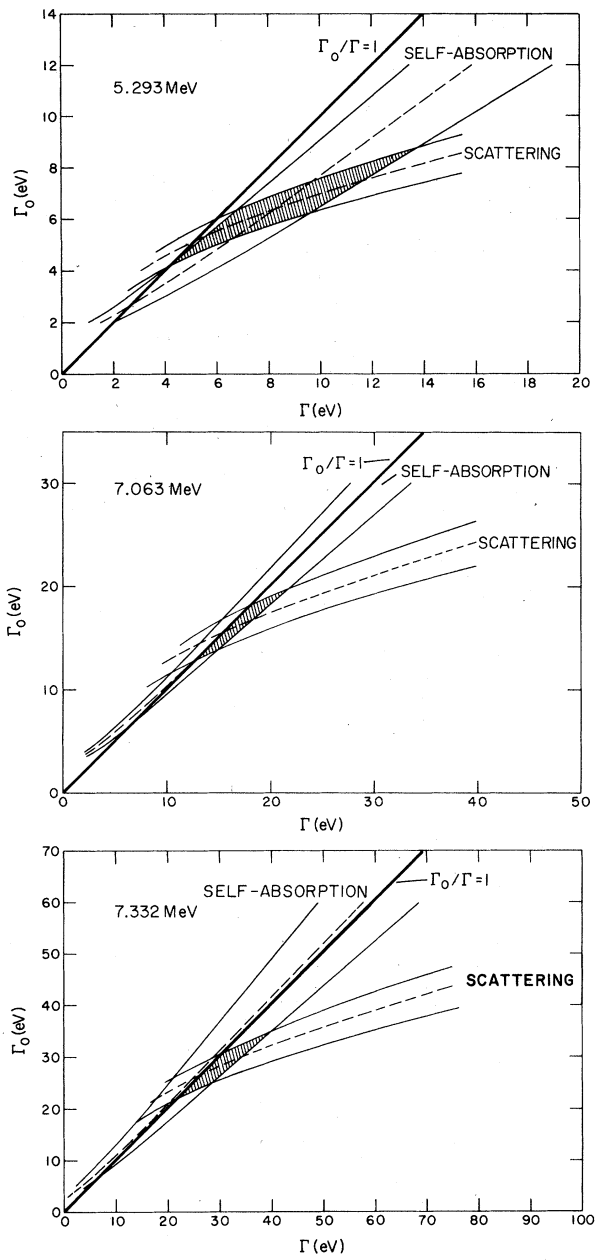

FIG. 8. Results of the self-absorption and scattering measurements for the ^{208}Pb levels at 5.293, 7.063, and 7.332 MeV. See Fig. 7 caption for explanation.

measurements but combining to contribute significantly to the tagged photon data. In both experiments, the 7 MeV doublet and the 7.332 MeV level were measured simultaneously, and their relative strengths should have been accurately determined. Since our sensitivity in Γ_0^2/Γ of levels near 7.3 MeV is ~1.5 eV, a number of small levels are required to explain the additional strength in this region.

This pattern of results is well supported by the Giessen data, and is also reflected in the relative strengths reported by Knowles *et al.*[42] (column 5 of Table V) for the levels at 6.720, 7.063, 7.083, and 7.332 MeV. However, this latter experiment, along with the work of Swann[37] and of Yeh and Lancman[44] (columns 6 and 7), indicates much more strength in the doublet than was observed with tagged photons or in two other experiments.[45,46] Our own $N_{\rm inc}(E)\epsilon(E)$ calibration measurements[18] show that such a large strength for the doublet is inconsistent with the reported widths for nearby levels in ^{31}P at 7.139 MeV and in ^{16}O at 6.912 and 7.117 MeV (Γ_0= 0.11 and 0.055 eV, respectively[48]).

The tagged photon work also detected strength (Γ_0^2/Γ= 4.4 eV) near 5.85 MeV, where we found no strong levels (weak levels would be obscured by known ^{206}Pb transitions), and near 6.26 MeV (Γ_0^2/Γ= 8.9 eV), largely explained by the levels at 6.262, 6.312, and 6.363 MeV. The weak transition which we observed at 7.278 MeV corresponds in energy to an M1 transition known from scattering experiments using ^{56}Fe(n,γ) photon sources[43]; our larger value for the width could indicate that we also excited another nearby level not reached with the highly monochromatic (n,γ) beam. Finally, the absence of strong peaks in the spectrum at 6.972 and 7.201 MeV is consistent with the recent $M2$ assignments for levels observed at these energies[49] in back angle (e,e') experiments at Darmstadt. $M1$ transitions with the reported widths and reasonable branching ratios would be easily visible in the spectrum shown in Fig. 5.

Table VI summarizes measurements of the branching ratios. The results listed in the second column are from a $(p,p'\gamma)$ experiment.[50] The listed errors are statistical; the reported possible systematic errors are 25%. The extremely small branching ratio reported here for the 6.720 MeV transition may imply that it is not the same level excited by photon scattering. The branching ratio of 0.5 attributed to a level at 7.09 MeV could correspond to either or both members of the doublet. The self-absorption measurement by Swann[37] of Γ_0/Γ= 0.8 was based on the combined scattering from both levels and is inconsistent with a branching ratio of 0.5, while a ratio of 1.0 cannot be ruled out by the data. The resonance fluorescence production experiment by Scholz[45] does yield a low value for the 7.083 MeV level, although the ascribed errors are quite large. Our own self-absorption results indicate branching ratios close to unity for all of the levels observed.

It has been suggested[51] that the level at 4.842 MeV corresponds to an unresolved doublet of 1^- and 1^+ states (with a spacing of $\lesssim$3 keV). Γ_0 $2.38^{+.52}_{-.27}$ eV was reported as the weighted aver-

TABLE V. Comparison of measured level widths for ^{208}Pb. The listed results from Ref. 35 have been renormalized from the values originally reported; see text for discussion.

Energy (MeV)	Γ_0^2/Γ[a] (eV)	Γ_0^2/Γ[b] (eV)	Γ_0^2/Γ[c] (eV)	Γ_0^2/Γ[d] (eV)	Γ_0^2/Γ[e] (eV)	Γ_0^2/Γ (eV)	Γ_0^2/Γ (eV)	Γ_0^2/Γ (eV)
4.085	0.68±0.15	0.51±0.20				0.49±0.05[f]		
4.842	5.0 ±0.8	6.3 ±2.2		6.9±1.4	6±2	5.1 ±0.8[g]		
5.293	5.1 ±0.8	8.6 ±3.0	4.6±0.7	7.0±1.4	7±2			
5.512	22.3 ±3.4	28 ±10	19.4±1.0	21.4±2.2	18±3			
5.948	1.0 ±0.3							
6.262	2.6 ±0.5	4.1 ±1.8	4.4±0.9					
6.312	3.2 ±0.6	1.0[m]						
6.363	1.6 ±0.4	0.5[m]						
6.720	7.6 ±1.5	15 ±6	7.2±0.6	13.0±1.6	13±3			
7.063	15.7 ±2.6	29 ±10	(16.9)[n]	25.9±2.1	24±3	31 ±3[h]	29±3[i]	18 ±3[j]
7.083	8.8 ±1.5	14 ±5	7.4±0.8		15±3	17 ±2[h]	16±3[i]	9.8[k]
7.243	1.7 ±0.6							
7.278	1.7 ±0.6							0.78±0.06[l]
7.332	26.9 ±4.8	38 ±13	25.5±1.3	44.5±2.9	42±1			

[a] This work.
[b] Reference 10.
[c] Reference 35.
[d] Reference 31.
[e] Reference 42.
[f] Reference 36.
[g] Reference 32.
[h] Reference 37.
[i] Reference 44.
[j] Reference 46.
[k] Reference 45; $\Gamma = 26^{+35}_{-12}$ eV, $\Gamma_0 = 16^{+6}_{-4}$ eV.
[l] Reference 43.
[m] Uncertainties "in excess of 50%."
[n] Value used for normalization of incident photon spectrum.

TABLE VI. Comparison of measured branching ratios for ^{208}Pb.

Energy (MeV)	Γ_0/Γ[a]	Γ_0/Γ[b]	Γ_0/Γ[c]	Γ_0/Γ[d]	Γ_0/Γ[e]	Γ_0/Γ[f]
4.842	$0.85^{+0.13}_{-0.09}$			1.0[h]		
5.293	$0.78^{+0.22}_{-0.14}$	0.80 ±0.08		1.0[h]		
5.512	$0.98^{+0.02}_{-0.04}$	0.78 ±0.07		1.0[h]		
6.720	$1.00^{+0.00}_{-0.11}$	0.067±0.008				
7.063	$0.98^{+0.02}_{-0.07}$		0.80[g]		$0.9^{+0.1}_{-0.4}$	
7.083	1.0[g]	0.50±0.04[g]			$0.8^{+0.2}_{-0.3}$	0.62[i]
7.332	$1.00^{+0.00}_{-0.12}$					

[a] This work; listed uncertainties are statistical only.
[b] Reference 50.
[c] Reference 37.
[d] Reference 52.
[e] Reference 44.
[f] Reference 45.
[g] See text for discussion.
[h] Uncertainties reported as 20–40 %.
[i] $\Gamma = 26^{+35}_{-12}$ eV, $\Gamma_0 = 16^{+6}_{-4}$ eV.

age of the values of Γ_0 determined in three self-absorption measurements (including one using a heated absorber, $T = 300°$ C, $\Delta = 3.4$ eV), compared with the scattering measurement value of $\Gamma_0^2/\Gamma = 4.9 \pm 0.5$ eV. The argument made was that since these results are inconsistent for a single level with $\Gamma_0/\Gamma \leq 1$, the existence of two levels with $\Gamma_0 \approx 2.5$ eV is indicated. Our own results for the 4.842 MeV level (at room temperature, $\Delta = 2.5$ eV), shown graphically in Fig. 7, do not require such an assumption. A large range of ground state decay widths are consistent with both the scattering and the self-absorption measurements. As indicated in Fig. 7 one cannot extract a value of Γ_0 from the absorption measurement alone (i.e., we are not in the regime $\Delta/\Gamma \gg 1$). If we assume $\Gamma_0/\Gamma = 1$, our absorption results yield $\Gamma_0 = 2.8^{+1.0}_{-0.5}$, which indeed does not agree with the scattering measurement. However, there is a range of consistent solutions for Γ_0 corresponding to values of $0.79 < \Gamma_0/\Gamma < 0.98$.

A number of other experiments have been performed which yield complementary information about the levels excited in photon scattering from ^{208}Pb. Assignments of natural parity have been made for almost all of the strongly excited levels[49,52-55] including the state at 7.063 MeV, suspected until recently of being an important part of the $M1$ giant resonance. Several conflicting measurements exist for the parity of the level at 4.842 MeV. Originally reported to be a 1^+ state on the basis of photon scattering polarization measurements at Bartol,[32] a $J^\pi = 1^-$ assignment was favored by (α, α') measurements.[53] Later Bartol photon scattering results[51] were inconsistent with either a pure $E1$ or $M1$ assignment and, as noted above, suggested the possibility of a $J^\pi = 1^-, 1^+$ doublet. However, no evidence for such a 1^+ state has been found in recent 180° electron scattering measurements by Raman *et al.*[56] The weak transition at 7.279 MeV remains the only unchallenged $M1$ excitation[43] below the neutron threshold. Furthermore, although some dipole strength ($\Sigma\Gamma_0^2/\Gamma \lesssim 20$ eV) may remain unresolved within 1 MeV below the threshold, our data places an upper limit of $\Gamma_0^2/\Gamma \lesssim 1.5$ eV on any individual $M1$ or $E1$ transition yet to be found in this region. The existing evidence for $M1$ strength above the neutron threshold has been recently reviewed.[57]

Charged particle scattering[50,58,59] and transfer reactions[52,60,61] have been used to excite single particle and single hole states in the neighbors of ^{208}Pb and to identify the particle-hole configurations involved in particular excited states of the core. The levels most strongly excited in photon scattering, such as the state at 5.512 MeV, appear to have strongly mixed configurations. On the other hand, the 5.293 MeV state contains a large $|s_{1/2}p_{1/2}^{-1}\rangle$ neutron component, and most of the $|d_{3/2}p_{1/2}^{-1}\rangle$ neutron strength has been located[52,61] at about 5.94 MeV. This latter state may correspond to the excitation we observe at 5.948 MeV, which was too weak to be detected in previous photon scattering experiments.

A number of calculations have been performed which predict the location of electric dipole strength in ^{208}Pb. The pioneering work of Brown and Bolsterli[62] demonstrated with a simple "schematic" model that a giant resonance containing all of the dipole strength could be formed from a superposition of the simple particle-hole states mixed by the residual interaction. More realistic calculations[1-5] indicate that a few percent of the $E1$ strength remains in the region of the unperturbed particle-hole states (~5–9 MeV).

An interesting study by Harvey and Khanna[4] identified some of the elements of the calculations which are important in determining the predicted distribution of strength. In the schematic model, it is the approximation that all of the radial integrals (over the various particle-hole states) are identical which causes all of the dipole strength to be concentrated in the giant resonance; the more realistic approximations allow some strength to remain near the energies of the unperturbed excitations. In ^{208}Pb, the ~2 MeV difference in the mean energies of the proton and neutron particle-hole states can lead to a grouping of strength into two "mini resonances" made up of highly mixed proton and neutron particle-hole excitations, which could correspond to the concentrations of strength observed experimentally[31] in the lead region near 5 and 7 MeV. None of the strong states of Ref. 4 have more than 15% of any particular particle-hole component. Unfortunately, the position of the giant resonance and the distribution of strength at lower energies is also sensitive to the range of the Gaussian function used to describe the residual interaction.

Comparisons of several sets of calculational results with each other and with experimental data have been made,[31,42] and will not be repeated here. The calculations do not yet appear to warrant a quantitative comparison with the data in the energy region from 5–10 MeV. Nonetheless, it is clear that the detailed distribution of photon strength in this energy region in ^{208}Pb provides a difficult and sensitive test for calculations yet to be developed.

B. ^{207}Pb and ^{209}Bi

The experimental results for ^{207}Pb and ^{209}Bi are summarized and compared with previous measurements in Tables VII and VIII. Measurements were made at 127° on both nuclei using a 7.65 MeV elec-

TABLE VII. Comparison of measured level widths for ^{207}Pb. Values of $g\Gamma_0^2/\Gamma$ were extracted from the present experiment assuming dipole angular distributions. Uncertainties include statistical and calibration errors.

Energy[a] (MeV ± keV)	$g\Gamma_0^2/\Gamma$[a] (eV)	$g\Gamma_0^2/\Gamma$[b] (eV)	$g\Gamma_0^2/\Gamma$[c] (eV)
4.871 ± 2	7.1 ± 1.1	13[e,f]	3.6 ± 0.5
4.981 ± 2	6.1 ± 1.2	7[f]	4.0 ± 0.5
5.489 ± 2	11.4 ± 1.9	12[f]	
5.596 ± 2	9.0 ± 1.4	8[f]	
5.611 ± 2[d]	5.5 ± 0.9		
5.690 ± 2	3.0 ± 0.6		
5.714 ± 2	6.2 ± 1.2	3[f]	
5.734 ± 2	5.1 ± 1.1		
5.794 ± 4	2.4 ± 1.0		
6.179 ± 2[d]	3.3 ± 0.7		
6.542 ± 4	2.3 ± 0.6		
6.735 ± 4	2.7 ± 0.7		
6.749 ± 4	7.2 ± 1.4	<10[f]	
6.818 ± 4	5.1 ± 0.9		
7.306 ± 4	3.0 ± 0.8		

[a] This work.
[b] Reference 10.
[c] Reference 36.
[d] Possible inelastic transitions; see text for discussion.
[e] Contains contribution from an additional level; see text for discussion.
[f] Uncertainties "in excess of 50%."

tron beam. In addition a 7.00 MeV beam measurement was made for ^{207}Pb. The values of $g\Gamma_0^2/\Gamma$ were extracted assuming a dipole angular distribution.

We report fifteen levels in ^{207}Pb, including three above the (γ,n) threshold at 6.738 MeV. Figure 9 shows the ^{207}Pb spectra. The strong peaks observed at the energies of ^{208}Pb transitions are consistent with the 13% ^{208}Pb contaminant in the enriched ^{207}Pb target. The (~7 keV) energy resolution achieved is indicated by the essentially complete separation of the two levels at 5.596 and 5.611 MeV.

The spectra were examined for evidence of branching from the observed resonances to low-lying levels in ^{207}Pb. Only two excited states below 2 MeV can be reached by dipole or quadrupole transitions from levels excited in this experiment, the $\frac{5}{2}^-$ state at 570 keV and the $\frac{3}{2}^-$ state at 898 keV. Two cases of possible branching were observed, both involving the first excited state ($J^\pi = \frac{5}{2}^-$) at 570 keV. Decay of the resonance at 6.749 MeV to this state would produce an inelastic peak at 6.179 MeV. Comparison of the relative counting rates yields a branching ratio for the 6.749 MeV level of $\Gamma_0/\Gamma = 0.53 \pm 0.03$ if other branching can be ignored. An alternative possibility is that the peak at 5.611 MeV is produced by decay of a resonance at 6.179 MeV to the first excited state. This would imply a branching ratio for the 6.179 MeV level of $\Gamma_0/\Gamma = 0.29 \pm 0.03$.

TABLE VIII. Comparison of measured level widths for ^{209}Bi. Values of $g\Gamma_0^2/\Gamma$ were extracted from the present experiment assuming dipole angular distributions; uncertainties include statistical and calibration errors. Parentheses indicate tentative assignments; levels in brackets are probably unresolved multiplets.

Energy[a] (MeV ± keV)	$g\Gamma_0^2/\Gamma$[a] (eV)	$g\Gamma_0^2/\Gamma$[b] (eV)	$g\Gamma_0^2/\Gamma$[c] (eV)
3.980 ± 4	0.88 ± 0.31		0.82 ± 0.08
4.757 ± 2	2.7 ± 0.7		2.9 ± 0.5
4.797 ± 2	3.5 ± 0.9	10[d]	2.7 ± 0.5
4.831 ± 2	1.5 ± 0.3		1.4 ± 0.3
(5.183 ± 4)	0.9 ± 0.3		
5.236 ± 2	1.4 ± 0.3		
5.281 ± 2	5.5 ± 1.1	12 ± 5	
5.293 ± 2	2.2 ± 0.6		
5.314 ± 2	3.0 ± 0.9		
5.354 ± 4	3.3 ± 0.8		
{5.410}	3.3 ± 0.8	8.3 ± 3.7	
(5.424 ± 4)	1.7 ± 0.5		
5.440 ± 4	1.6 ± 0.5		
5.462 ± 4	1.4 ± 0.4		
5.485 ± 2	4.0 ± 0.8		
5.497 ± 2	4.8 ± 0.9	17 ± 6	
{5.509}	6.8 ± 1.2		
{5.536}	4.4 ± 1.0	6.6 ± 2.6	
5.554 ± 2	2.6 ± 0.8		
5.573 ± 4	1.7 ± 1.0		
5.590 ± 2	3.2 ± 0.9		
5.662 ± 2	1.6 ± 0.4		
(6.911 ± 4)	2.4 ± 0.5		
(6.945 ± 4)	2.1 ± 0.6		
6.983 ± 4	2.6 ± 0.5		
(7.106 ± 4)	1.0 ± 0.3		
7.171 ± 4	4.7 ± 1.0		
7.246 ± 4	3.7 ± 0.8		
7.264 ± 4	2.4 ± 0.9		
7.287 ± 4	2.6 ± 0.7		
7.360 ± 4	4.3 ± 1.1		

[a] This work.
[b] Reference 10.
[c] Reference 36.
[d] Uncertainty reported "in excess of 50%."

The comparison in Table VII of the present results with those from the earlier (MUSL-1) work of Coope *et al.*[10] shows reasonable agreement in most cases, in view of the increased sensitivity and precision of the newer measurements. The strength reported by Coope near 4.871 MeV included contributions from two partially resolved levels at 4.847 and 4.875 MeV. The lower of these is actually consistent in our data (both in energy and counting rate) with the 4.842 MeV transition in the ^{208}Pb target contaminant. Coope reported additional levels at 5.209 and 5.223 MeV, each with $g\Gamma_0^2/\Gamma = 8$ eV. We find no evidence for a transition at 5.209 MeV, while most of the yield at 5.223

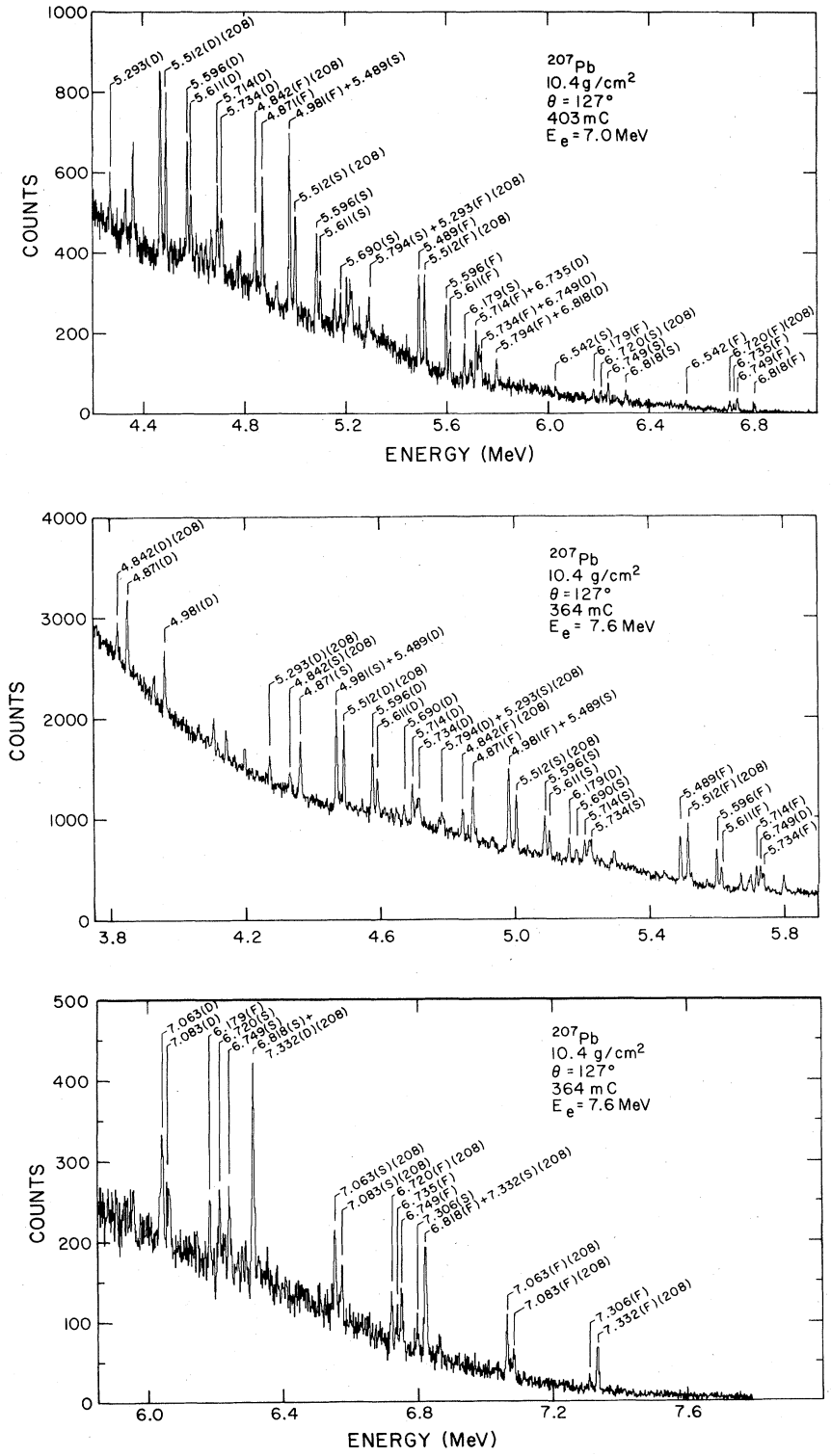

FIG. 9. Spectra for 7.0 MeV (upper figure) and 7.6 MeV (two lower figures) bremsstrahlung scattered at 127° from a cylindrical target of enriched (84.8%) ^{207}Pb. One channel corresponds to 1.36 keV in the 7.0 MeV spectrum and 1.48 keV in the 7.6 MeV data.

MeV is due to an escape peak from a newly resolved transition at 5.734 MeV. The spectrum does appear to show a level at 5.223 MeV (based on an apparent double escape peak) with $g\Gamma_0^2/\Gamma \sim 2.5$ eV, but a definite assignment has not been made due to inconsistencies in the escape peak ratios, which probably imply contributions from additional unidentified levels. Similar effects prevent extraction of reliable strengths for the apparent weak-coupling doublet observed by Swann[36] at 4.104 and 4.140 MeV (near the ^{208}Pb 4.085 MeV 2^+ state); the widths assigned to the 4.871 and 4.981 MeV levels in that experiment are smaller than our results (see Table VII).

Three levels have been observed above neutron threshold (6.738 MeV). Two, at 6.749 MeV ($g\Gamma_0^2/\Gamma = 7.2$ eV) and 6.818 MeV ($g\Gamma_0^2/\Gamma = 5.1$ eV), may correspond to small neutron resonances on ^{206}Pb observed[63] at 11.3 and 80.4 keV, respectively. The third, at 7.306 MeV ($E_n = 571 \pm 4$ keV) is close to neutron resonances observed at 570.8 and 572.4 keV. The former has the spin-parity assignment $J^\pi = \frac{5}{2}^+$, the latter $\frac{3}{2}^+$. Only $\frac{3}{2}^+$ would be viable for a photon transition to the ground state of ^{207}Pb($\frac{1}{2}^-$). No evidence was found for the existence of levels reported by Swann[37] at 7.186 and 7.206 MeV with $g\Gamma_0^2/\Gamma = 15$ and 25 eV, respectively (refer to Fig. 9).

Results from the more complicated ^{209}Bi spectrum are presented in Table VIII. Widths are given for 31 levels. As indicated, three appear to be unresolved multiplets, and another five are given tentative assignments because of insufficient yields or resolution. The spectrum obtained (in 48 hours) with a 7.6 MeV beam is shown in Fig. 10, where only some of the more prominent peaks are labeled. A high density of rather weak levels ($g\Gamma_0^2/\Gamma \sim 3$ eV) is found in the region from 5.2 to 5.6 MeV, while another grouping of states above 7 MeV is barely observable above the background. Since a large concentration of strength is known to be present near 7 MeV from the tagged photon measurements[31] (see Sec. IV D), this strength must be shared among a very large number of weak levels.

A search was made for branching of the observed resonances to low-lying levels. Only two states in ^{209}Bi below 2.5 MeV of excitation have the proper spin and parity to be reached by dipole or quadrupole decays. These are the first two excited states, at 896 keV ($J^\pi = \frac{7}{2}^-$) and at 1.608 MeV ($J^\pi = \frac{13}{2}^+$). No evidence of inelastic transitions to these states was found.

The present results are compared with the measurements of Coope *et al.*[10] and of Swann[36] in Table VIII. The energies originally reported by Swann for the three levels near 4.8 MeV were later increased by 11 keV (Ref. 64); these values agree well with our measurements. However, all of our energies (which have been checked and remeasured) are systematically ~12 keV lower than those reported by Coope *et al.* All three experiments are in good agreement for the widths of the levels listed below 5 MeV. Swann reports five additional levels near 4 MeV with $g\Gamma_0^2/\Gamma \sim 0.3$ eV, which are too weak to have been distinguished by us. Additional levels seen by Coope at 4.228 and 4.501 MeV with $g\Gamma_0^2/\Gamma \sim 3$ eV were not reported by Swann and are not supported by our data. At higher energies, the present results are generally consistent with the older measurements within the experimental errors.

Swann has also reported levels in ^{209}Bi at 7.179 and 7.202 MeV with $g\Gamma_0^2/\Gamma = 24$ and 30 eV, respectively.[37] The first of these could correspond to our level at 7.171 MeV (particularly since energies measured for the nearby ^{208}Pb doublet in the same experiment are ~7 keV higher than our values). However, we measure $g\Gamma_0^2/\Gamma = 4.7$ eV for this level and find no evidence of a strong level near 7.20 MeV, as seen in Fig. 10. Wolf *et al.*,[65] using neutron capture photons, report an $M1$ transition at 7.168 MeV with a branching ratio of 1 and $\Gamma_0 = 0.82 \pm 0.04$ eV. This only accounts for part of the strength we observe at 7.171 MeV, perhaps indicating contributions from another level not excited within the ~10 eV energy spread of the (n,γ) photon beam.

The results for ^{207}Pb and ^{209}Bi are summarized in Fig. 11, along with the widths determined for ^{208}Pb and ^{206}Pb (to be discussed in Sec. IV C). Both the ^{207}Pb and the ^{209}Bi spectra show a considerably greater density of (weaker) levels than is observed in ^{208}Pb, a feature interpretable as a fragmentation of the strength resident in the ^{208}Pb core by the additional hole or particle.

It is interesting to consider whether the weak coupling model[7] gives a viable explanation for the levels which we observe.[10,36,37] ^{209}Bi and ^{207}Pb are represented in this model as a ^{208}Pb core plus a proton or a neutron hole. One then expects excited states in these nuclei from excitations of the core and of the valence particle (or hole). For example, a 1^- core excitation coupled to the valence particle in its lowest energy orbit would produce a doublet in ^{207}Pb ($p_{1/2} \oplus 1^- \rightarrow \frac{1}{2}^+, \frac{3}{2}^+$) and a triplet in ^{209}Bi ($h_{9/2} \oplus 1^- \rightarrow \frac{7}{2}^+, \frac{9}{2}^+, \frac{11}{2}^+$). The energy splitting of the multiplet and any shift of its centroid would depend on the strength of the coupling of the particle to the core excitation. The cross section for exciting a member of the multiplet would be related to its spin I according to the $(2I+1)$ rule; the total strength $\sum g\Gamma_0$ in the multiplet would equal that in the core transition.

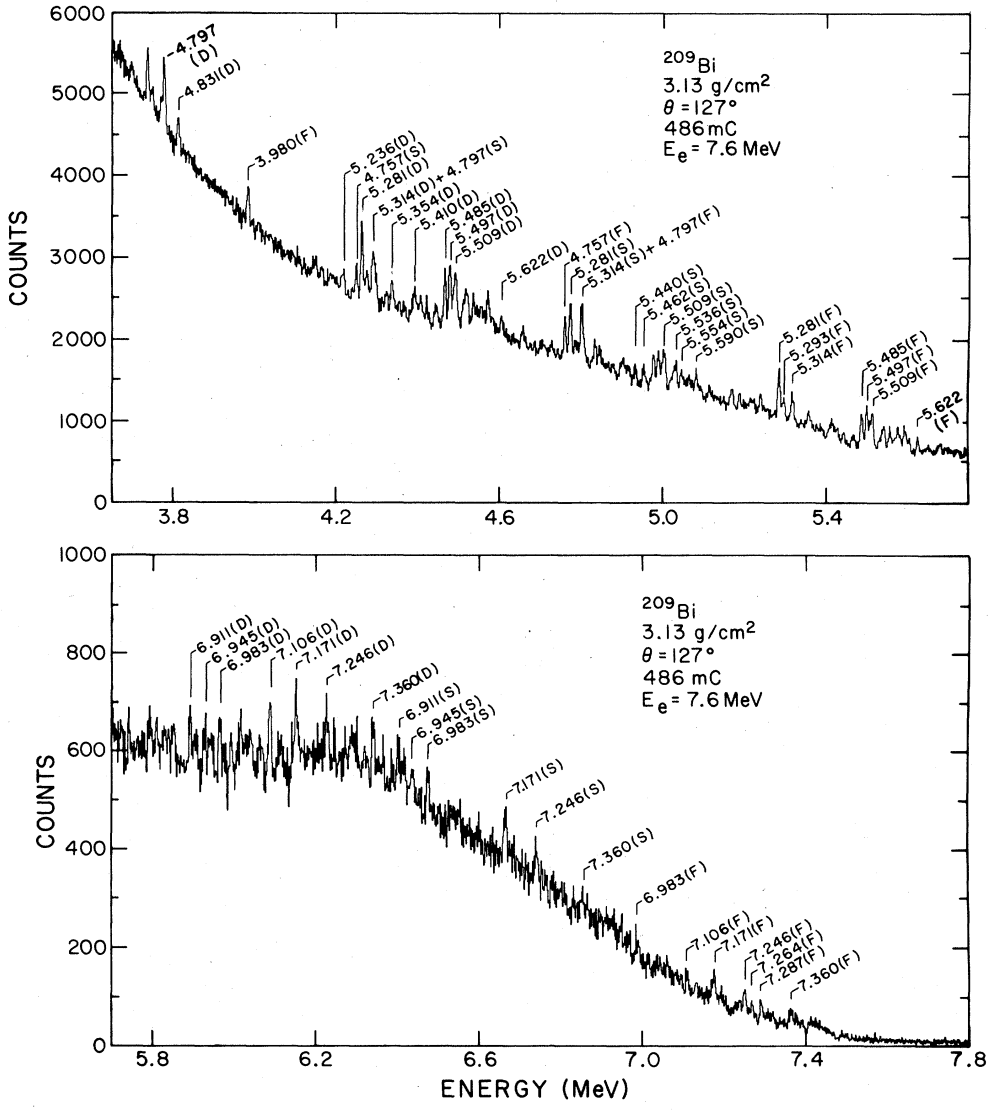

FIG. 10. Spectrum for 7.6 MeV bremsstrahlung scattered at 127° from a natural bismuth target (100% ^{209}Bi). One channel corresponds to 1.42 keV.

This simple scheme has been successful in explaining the properties of the doublet in ^{207}Pb and the septuplet in ^{209}Bi corresponding to the first excited state of the ^{208}Pb core (the 2.614 MeV octupole vibration), and has also been applied to other collective core excitations above 4 MeV.[66-68] However, there are various instances in which such a simple pattern might not occur. For example, if the wave function of the excited core contained significant components which overlapped with the valence particle (hole) orbit, then the coupling would not in general be weak. Also, if there were nearby levels of the same spin and parity, a mixing of these states with the weak coupling multiplets would be expected. Such circumstances could alter the spacing or energy centroid of the multiplet, reduce the strength observed in one or more members, or distort the simple pattern completely.

Looking at the summary of the levels drawn in Fig. 11, one can see obvious candidates for weak coupling multiplets near the lowest 1$^-$ transition in ^{208}Pb at 4.842 MeV. The levels in ^{207}Pb at 4.871 and 4.981 MeV have a combined $g\Gamma_0^2/\Gamma$ of 13.2 eV compared to 15 eV for the core transition. The three levels in ^{209}Bi at 4.757, 4.797, and 4.831 MeV are rather weaker, comprising a total $g\Gamma_0^2/\Gamma$ of 7.7 eV. Of course, the branching ratios for the states in ^{207}Pb and ^{209}Bi have not been sensitively measured, preventing a direct comparison

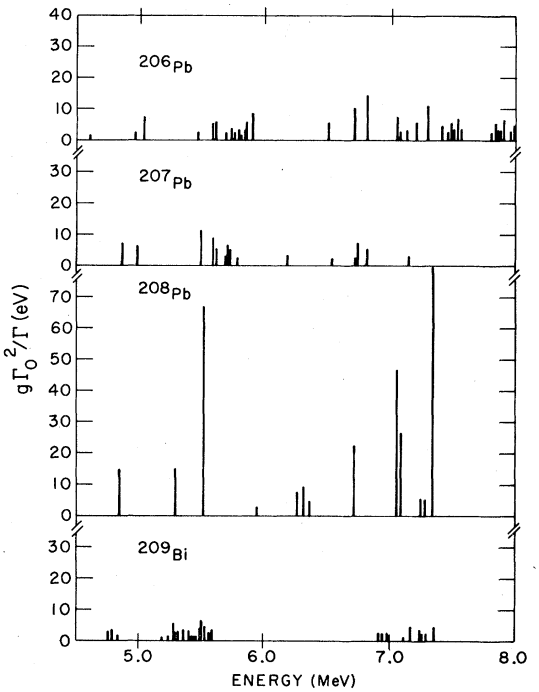

FIG. 11. Summary of the values of $g\Gamma_0^2/\Gamma$ for levels in ^{206,207,208}Pb and ^{209}Bi measured in this experiment.

of the strengths ($g\Gamma_0$). The spins and parities of the levels in these supposed multiplets are also not known. Nevertheless, these data suggest a weak coupling interpretation.

Near the next strong 1^- core transition at 5.293 MeV, no levels are observed in ^{207}Pb; the $p_{1/2}$ neutron hole should not be expected to couple weakly to the core transition, which contains a large $|s_{1/2}p_{1/2}^{-1}\rangle$ component. In ^{209}Bi a closely spaced triplet is found centered at this energy (5.281, 5.293, and 5.314 MeV) with a combined $g\Gamma_0^2/\Gamma$ of 10.7 eV, or about 70% of that measured for the core transition.

Near the energy of the ^{208}Pb transition at 5.512 MeV, a number of levels are observed in both ^{207}Pb and ^{209}Bi, but no strong doublet or triplet stands out. In fact, no more than 30% of the core strength is evident in any two levels in ^{207}Pb or in any three levels in ^{209}Bi near this energy. At higher energies in ^{207}Pb, a closely spaced doublet is observed at 6.735 and 6.749 MeV with $g\Gamma_0^2/\Gamma$ about 40% as large as that for the 6.720 MeV core transition; the other ^{208}Pb levels are above the ^{207}Pb(γ,n) threshold. In ^{209}Bi there are no strong triplets near any of the core states above 5 MeV.

The absence of a simple multiplet structure in the spectra of ^{207}Pb and ^{209}Bi corresponding to the higher energy ^{208}Pb transitions may indicate the mixing of weak coupling configurations with other levels. The weak coupling model itself predicts many additional states at nearby energies, built on combinations of (lower energy) core excitations with excitations of the valence particle (hole) to higher orbitals. With increasing energy, the higher density of levels with the appropriate spin and parity must eventually perturb the simple weak coupling patterns seen in the low energy spectra.

C. ^{206}Pb

The experimental results for ^{206}Pb are summarized in Table IX. Spins of 29 levels were determined by measurements at 90° and 127° using an 8.50 MeV electron beam. Values of Γ_0^2/Γ for 38 levels were extracted from the 127° data, assuming dipole transitions for levels whose spins were not measured. As noted in Table IX, five of these levels appear to be unresolved multiplets, two are given tentative assignments and the reported widths for three others may include contributions from additional transitions which could not be identified. The 127° spectrum is shown in Fig. 12 and the 90° spectrum in Fig. 13. Figure 12 shows the high density of weak levels between 5.5 and 6.0 MeV; the strongest level observed below 6 MeV is at 5.903 MeV, with $\Gamma_0^2/\Gamma = 3$ eV. Nearby, at 5.512 MeV, a peak due to the strong ^{208}Pb transition is clearly visible, despite the fact that the ^{208}Pb contaminant comprises only 3% of the target. On the other hand, most of the yields at 6.724, 7.062, and 7.078 MeV are due to transitions in ^{206}Pb rather than ^{208}Pb.

The results of the angular distribution measurements are presented in Table X; the quoted errors are statistical only. The ratio determined for the known quadrupole transition[69] at 4.115 MeV is just consistent with the solid angle averaged quadrupole ratio of 2.20, and is much higher than the other measurements, which are all consistent with the dipole ratio of 0.73.

A search was made for inelastic peaks produced by branching of the observed resonances to the five levels of appropriate spin and parity below 2 MeV in ^{206}Pb [0.803($J^\pi = 2^+$), 1.165(0^+), 1.460(2^+), 1.704(1^+), and 1.784(2^+) MeV]. The results are summarized in Table XI. Four transitions below 5 MeV not reported in earlier elastic scattering experiments by Swann[36] coincide in energy with the inelastic decays indicated. Corresponding branching ratios of the resonances were calculated assuming no other channels were significant. The listed uncertainties are statistical only; systematic errors may be significant, particularly due to the large background at these energies. Three additional lines above 6.5 MeV (not observed previously) are possible inelastic transitions, al-

TABLE IX. Comparison of measured level widths for ^{206}Pb. Values of Γ_0^2/Γ were extracted from the present experiment assuming dipole transitions for levels whose spins were not measured; uncertainties include statistical and calibration errors. Parentheses indicate tentative assignments; levels in brackets are probably unresolved multiplets.

Energy[a] (MeV ± keV)	J^a	Γ_0^2/Γ^a (eV)	Γ_0^2/Γ^b (eV)	Γ_0^2/Γ^c (eV)
4.115 ± 2	2	0.58 ± 0.15		0.30 ± 0.06
4.329 ± 4	1	0.48 ± 0.11		0.90 ± 0.09
4.604 ± 4		0.58 ± 0.16		0.23 ± 0.03
4.972 ± 2	1	0.95 ± 0.23	0.8 ± 0.3	0.8 ± 0.2
5.038 ± 2	1	2.6 ± 0.4	1.6 ± 0.6	2.3 ± 0.5
5.470 ± 4		0.7 ± 0.2		
5.580 ± 2	1	1.7 ± 0.3	0.5[f]	
5.615 ± 2	1	1.8 ± 0.4	1.0[f]	
5.692 ± 4	1	0.8 ± 0.2	0.5[f]	
5.732 ± 2[d]	1	1.3 ± 0.3		
5.760 ± 4	1	0.9 ± 0.2		
5.798 ± 4[d]		1.1 ± 0.3	1.0[f]	
5.816 ± 4		0.5 ± 0.2		
5.846 ± 2	1	1.1 ± 0.2	3.0[f]	
5.857 ± 2	1	2.0 ± 0.4		
5.903 ± 2	1	3.0 ± 0.6	4.4 ± 1.8	
6.509 ± 2[e]	1	1.9 ± 0.4		
6.724 ± 4	1	3.4 ± 0.6	5.5 ± 2.2	
6.820 ± 2	1	4.7 ± 0.9	7.4 ± 3.0	
7.062 ± 4	1	2.5 ± 0.6		
7.078 ± 4[e]	1	0.9 ± 0.3		
(7.127 ± 2)		1.0 ± 0.2		
(7.202 ± 4)[e]	1	1.8 ± 0.4		
{7.310}	1	3.7 ± 0.9		
7.423 ± 4	1	1.6 ± 0.4		
7.464 ± 4		0.9 ± 0.4		
7.487 ± 4[d]		1.7 ± 0.4		
7.506 ± 2	(1)	1.2 ± 0.4		
7.543 ± 2	1	2.3 ± 0.6		
7.570 ± 4	1	1.1 ± 0.5		
{7.815}		0.8 ± 0.2		
{7.846}	1	1.9 ± 0.4		
7.880 ± 2	1	1.1 ± 0.3		
7.891 ± 4	1	1.6 ± 0.4		
7.903 ± 4	1	2.2 ± 0.5		
7.972 ± 4	1	1.0 ± 0.3		
{8.000}	1	1.6 ± 0.4		
{8.040}		0.27 ± 0.09		

[a] This work.
[b] Reference 10.
[c] Reference 36.
[d] May include contribution from an additional level.
[e] May be an inelastic transition; see text and Table XI.
[f] Uncertainty reported "in excess of 50%."

though the resulting branching ratios are quite small in all but one case. They are listed in Table XI, but have also been analyzed as elastic peaks and listed in Table IX. Finally, an additional eight transitions known to be elastic (from preliminary data with a 7.6 MeV beam, and from the results of Swann and Coope *et al.*) coincide in energy with possible inelastic decays from higher excitations which could affect the widths quoted for these levels in Table IX.

Table IX also compares the present results with earlier work (Refs. 10 and 36). The new results are in very good agreement with the widths reported by Swann for levels at 4.972 and 5.038 MeV, but there are large and rather erratic discrepancies for the three lower energy levels. In the case of the 4.115 MeV transition this could be due to an inelastic contribution as discussed above, but the discrepancy for the 4.329 MeV level is in the opposite direction. At higher energies, the new results generally agree within the experimental errors with the widths reported by Coope *et al.*

D. Distribution of photon strength in the lead region

Our measurements of $g\Gamma_0^2/\Gamma$ for discrete levels in all four nuclei have been summarized in Fig. 11. For a more complete description of the distribution of photon strength, we can combine our results with the complementary low resolution measurements of Laszewski and Axel.[31] The latter experiment employed tagged photon beams (with energy resolution from 50 to 150 keV) to measure the energy-averaged elastic scattering cross sections. The tagged photon data include contributions from small levels not visible above our backgrounds, while the higher resolution experiment provides a more detailed account of the distribution of strength among the stronger levels.

The integral of the elastic scattering cross section over an $E1$ resonance can be related to the ground state decay width and the reduced transition probability as follows (for a thin target):

$$\int \sigma_{\gamma\gamma}(E)dE = \pi^2(\hbar c)^2 \frac{1}{E^2}\frac{g\Gamma_0^2}{\Gamma} = \frac{16\pi^3}{9(\hbar c)}\frac{\Gamma_0}{\Gamma} EB(E1\uparrow). \quad (7)$$

The classical $E1$ sum rule for ^{208}Pb gives $\sum E_i B_i(E1\uparrow) = 735\ e^2\,\mathrm{fm}^2\,\mathrm{MeV}$, corresponding to an integrated total cross section of about 3000 MeV mb.[31] Figure 14 compares the values of $g\Gamma_0^2/\Gamma \cdot 1/E^2$ determined in the present experiment with the corresponding average photon scattering cross sections[31] (which, except for ^{208}Pb, have not been corrected for target resonant absorption).

Figure 14 shows that the photon strength below neutron threshold in all four nuclei is concentrated into two energy regions near 5.5 and 7.0 MeV. As an estimate of the $E1$ strength in each region, the integrated elastic scattering cross sections[31] from

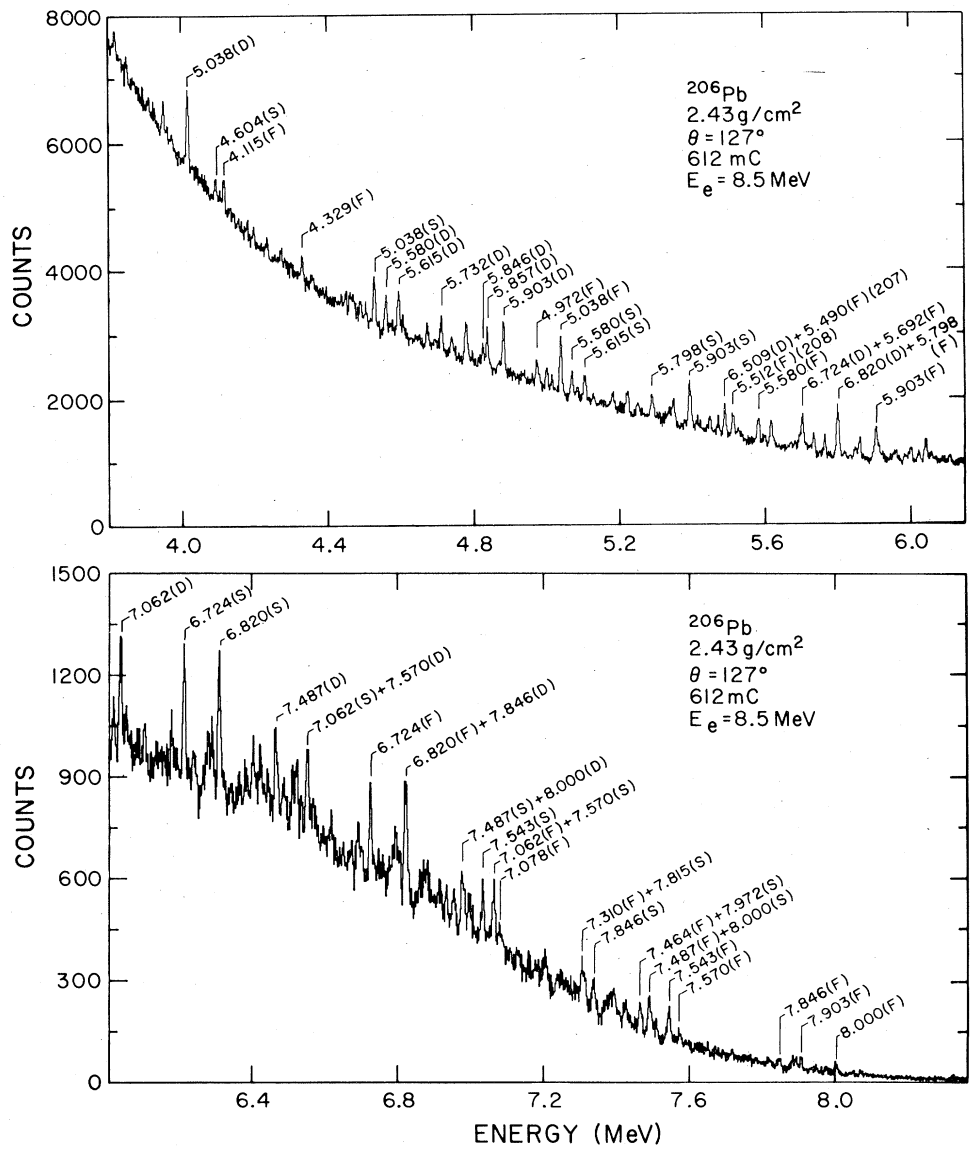

FIG. 12. Spectrum for 8.5 MeV bremsstrahlung scattered at 127° from an enriched (88%) ^{206}Pb target. One channel corresponds to 1.47 keV.

5.0 to 6.0 MeV and from 6.5 to 7.5 MeV are listed in Table XII; these results have been corrected for nuclear absorption, and each would be proportional to $B(E1\uparrow)$ if all levels were $E1$ having ground state branching ratios of one. The integrated cross section for ^{208}Pb is 15 MeV mb near 5.5 MeV and 24 MeV mb near 7.0 MeV, corresponding to a total of about 1.3% of the dipole sum rule. The photon strength in ^{208}Pb is dominated by the strong transitions found in the present experiment; 86% and 76% of the integrated cross sections near 5.5 and 7.0 MeV, respectively, is explained by the levels which we observed. Most of the discrepancy near 7.0 MeV comes from additional strength observed in the low resolution work near the 6.720 and 7.332 MeV states.

The integrated cross sections are quite similar for all four nuclei in these two regions; the differences (shown in Table XII) may be due simply to an expected increase in branching in nuclei away from the doubly closed shell. In the ^{206,207}Pb isotopes, the strength near 5.5 MeV is shifted to slightly higher energy and fragmented into a number of levels. In both cases, about 50% of the total strength is contained in levels with $g\Gamma_0^2/\Gamma > 1$ eV; seven such levels are found in ^{207}Pb and 11 in

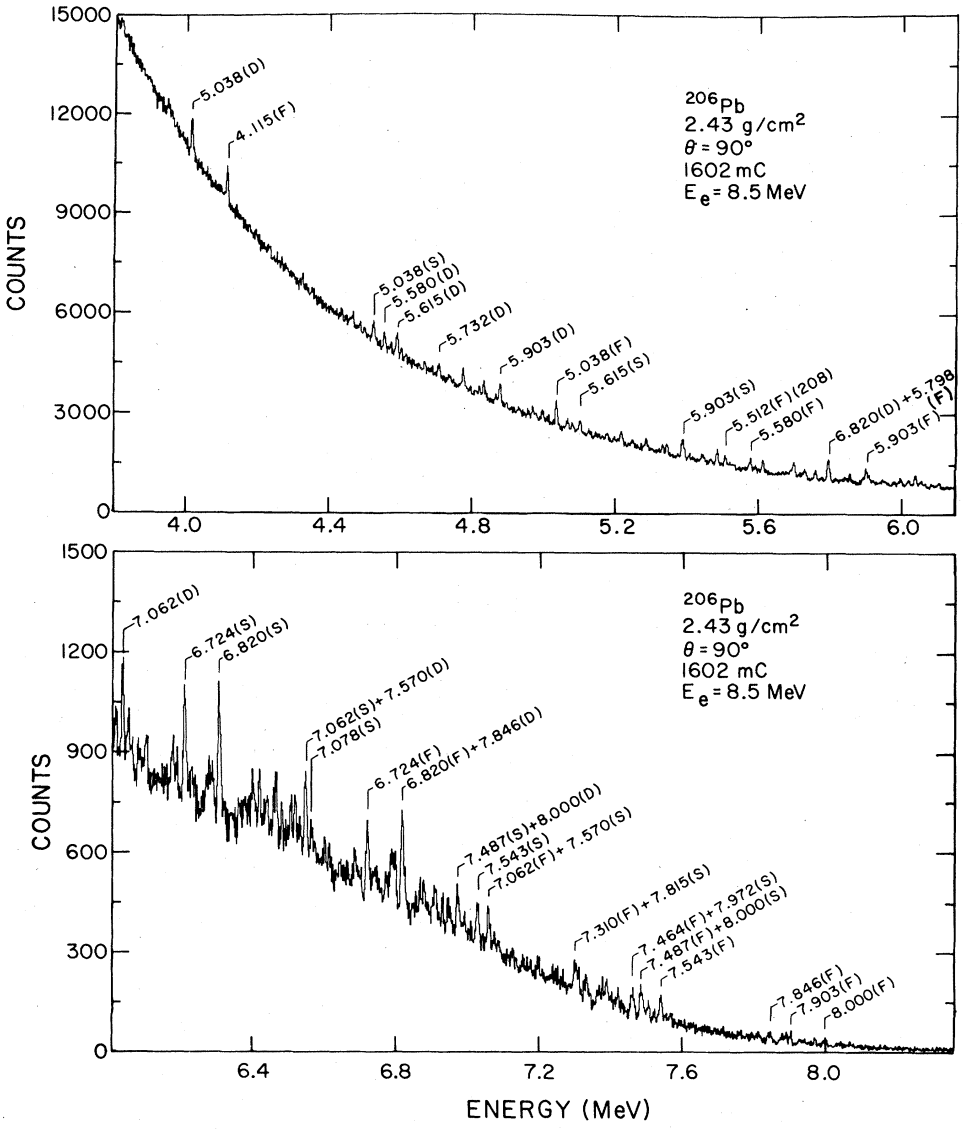

FIG. 13. Spectrum for 8.5 MeV bremsstrahlung scattered at 90° from an enriched (88%) ^{206}Pb target. One channel corresponds to 1.47 keV.

^{206}Pb. In ^{209}Bi almost 80% of the strength near 5.5 MeV was resolved, split into a relatively uniform distribution of 17 levels spread over ~350 keV, with strengths from 1 to 7 eV.

No levels at all are distinguished in bismuth over an interval of more than one MeV between the two major concentrations of strength. Near 7 MeV, the average cross section shows a rather featureless bump corresponding to a large number of very weak levels. Only about 23% of the integrated cross section in this region is explained by the 9 levels which we observed. Assuming a Porter-Thomas distribution of level widths[70] and an experimental sensitivity of 1 eV, these results indicate that the average level spacing for $E1$ excitations near 7 MeV in bismuth is approximately 2 keV. In the same energy region, the ^{206}Pb cross section exhibits considerable structure, including peaks correlated in energy with the concentrations of strength in the ^{208}Pb core. The discrete levels observed in the present experiment tend to cluster near the corresponding energies; about 35% of the ^{206}Pb strength in this region is resolved into 25 levels with $\Gamma_0 > 1$ eV. These results along with an estimate of 1 eV for the experimental sensitivity imply an average spacing of about 4.5 keV for $E1$

TABLE X. ^{206}Pb angular distribution measurements. Listed uncertainties are statistical only.

Energy (MeV)	$W(90°)/W(127°)$	J
4.115	1.76±0.44	2
4.329	0.69±0.17	1
4.972	0.60±0.16	1
5.038	0.69±0.06	1
5.580	0.67±0.14	1
5.615	0.81±0.13	1
5.692	0.65±0.19	1
5.732	0.81±0.15	1
5.760	0.69±0.18	1
5.846	0.73±0.22	1
5.857	0.66±0.09	1
5.903	0.67±0.09	1
6.509	0.74±0.17	1
6.724	0.76±0.13	1
6.820	0.81±0.16	1
7.062	0.80±0.19	1
7.078	0.90±0.25	1
7.202	0.70±0.22	1
7.310	0.69±0.19	1
7.423	0.84±0.26	1
7.506	1.11±0.54	(1)
7.543	0.73±0.21	1
7.570	0.82±0.53	1
7.846	0.85±0.20	1
7.880	0.88±0.37	1
7.891	0.84±0.23	1
7.903	0.79±0.19	1
7.972	0.92±0.45	1
8.000	0.91±0.26	1

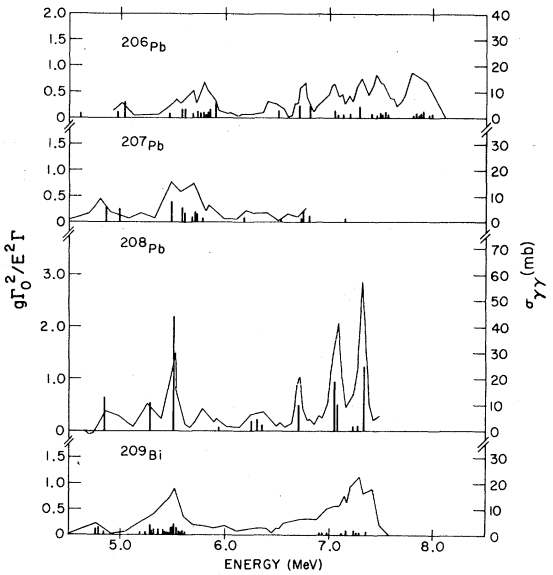

FIG. 14. Comparison of the present results with average elastic scattering cross section measurements. Bars whose heights represent the values of $(1/E^2)\times(g\Gamma_0^2/\Gamma)$ for levels observed in this experiment are superimposed on the low resolution (tagged photon) measurements of Laszewski and Axel (Ref. 31).

transitions in ^{206}Pb near 7 MeV.

This work was based on a Ph.D. thesis submitted to the University of Illinois by T. Chapuran. A preliminary account of some of the results ap-

TABLE XI. Possible branching in ^{206}Pb. See text for discussion. All uncertainties are statistical only.

Energy (MeV)		Possible branch	Γ_0/Γ
		Apparent inelastic peaks	
4.196		5.903 → 1.704(1^+)	0.76±0.06
4.235		5.038 → 0.803(2^+)	0.80±0.05
	or	5.692 → 1.460(2^+)	0.53±0.09
4.272		5.732 → 1.460(2^+)	0.68±0.07
4.356		5.816 → 1.460(2^+)	0.42±0.14
		Other possible inelastic peaks	
6.509		7.310 → 0.803(2^+)	0.56±0.06
	or	7.972 → 1.460(2^+)	0.18±0.04
7.078		7.880 → 0.803(2^+)	0.36±0.06
7.202		8.000 → 0.803(2^+)	0.32±0.05
		Inelastic transitions which coincide in energy with known elastic peaks	
4.115		5.816 → 1.704(1^+)	
4.329		5.490 → 1.165(0^+)	
5.036		6.820 → 1.784(2^+)	
5.615		7.078 → 1.460(2^+)	
5.693		7.423 → 1.460(2^+)	
5.760		7.464 → 1.704(1^+)	
5.798		7.506 → 1.704(1^+)	
6.724		7.891 → 1.165(0^+)	

TABLE XII. Transition strength comparison near 5.5 and 7 MeV. The average cross section measurements are from Ref. 31. See text for discussion.

Nucleus	$\int \sigma_{\gamma\gamma} dE$ (MeV mb)	% ^{208}Pb strength	% resolved
	5.0–6.0 MeV		
^{206}Pb	15.8	104%	52%
^{207}Pb	12.6	83%	52%
^{208}Pb	15.2	100%	86%
^{209}Bi	10.4	68%	79%
	6.5–7.5 MeV		
^{206}Pb	20.2	83%	35%
^{207}Pb			
^{208}Pb	24.4	100%	75%
^{209}Bi	10.7	44%	23%

peared in Ref. 71, which is superseded by the present report.

ACKNOWLEDGMENTS

We wish to thank Peter Axel for valuable discussions, and Lloyd Young and the MUSL-2 accelerator staff for providing the many hours of stable beam required for these experiments. This research, including the development and operation of MUSL-2 and its experimental areas, was supported by a grant from the U. S. National Science Foundation.

*Present address: Department of Physics, State University of New York, Stony Brook, New York, 11794.

[1]V. Gillet, A. M. Green, and E. A. Sanderson, Nucl. Phys. 88, 321 (1966).
[2]T. T. S. Kuo, J. Blomqvist, and G. E. Brown, Phys. Lett. 31B, 93 (1970).
[3]W. W. True, C. W. Ma, and W. T. Pinkston, Phys. Rev. C 3, 2421 (1971).
[4]M. Harvey and F. C. Khanna, Nucl. Phys. A221, 77 (1974).
[5]W. Knüpfer (private communication).
[6]G. E. Brown and J. Speth, *Neutron Capture Gamma-Ray Spectroscopy*, edited by Robert E. Chrien and Walter R. Kane (Plenum, New York, 1979), p. 181.
[7]A. Arima and I. Hamamoto, Annu. Rev. Nucl. Sci. 21, 55 (1971); A. de Shalit, Phys. Rev. 122, 1530 (1961).
[8]B. Arad and G. Ben-David, Annu. Rev. Nucl. Sci. 24, 35 (1974).
[9]P. Axel, A. O. Hanson, J. R. Harlan, R. A. Hoffswell, D. Jamnik, D. C. Sutton, and L. M. Young, IEEE Trans. Nucl. Sci. NS-22, 1176 (1975).
[10]D. F. Coope, L. E. Cannell, and M. K. Brussel, Phys. Rev. C 15, 1977 (1977).
[11]L. E. Cannell, Ph.D. thesis, University of Illinois, 1976 (unpublished).
[12]P. Axel *et al.*, IEEE Trans. Nucl. Sci. NS-24, 1133 (1977).
[13]F. R. Metzger, *Progress in Nuclear Physics* (Pergamon, Elmsford, New York, 1959), Vol. 7, p. 53.
[14]R. Moreh, O. Shahal, and I. Jacob, Nucl. Phys. A228, 77 (1974).
[15]R. Moreh, O. Shahal, and V. Volterra, Nucl. Phys. A262, 221 (1976).
[16]J. T. Routti and S. G. Prussin, Nucl. Instrum. Methods 72, 125 (1969).
[17]F. Ajzenberg-Selove, Nucl. Phys. A248, 1 (1975).
[18]T. Chapuran, Ph.D. thesis, University of Illinois, 1979 (unpublished).
[19]D. E. Alburger and D. H. Wilkinson, Phys. Rev. C 3, 1492 (1971).
[20]P. T. Kan, G. A. Peterson, D. V. Webb, S. P. Fivozinsky, J. W. Lightbody, Jr., and S. Penner, Phys. Rev. C 11, 323 (1975).
[21]E. Spamer and H. Artus, Z. Phys. 198, 445 (1967).
[22]E. Spamer, Z. Phys. 191, 24 (1966).
[23]O. Titze, Z. Phys. 220, 66 (1969).
[24]P. M. Endt and C. Van der Leun, Nucl. Phys. A214, 1 (1973).
[25]U. E. Berg, K. Wienhard, and H. Wolf, Phys. Rev. C 11, 1851 (1975).
[26]E. O. deNeijs, G. D. Haasbroek, M. A. Meyer, R. S. Rossouw, and D. Reitmann, Nucl. Phys. A254, 45 (1975).
[27]C. P. Swann, Bull. Am. Phys. Soc. 14, 1203 (1969).
[28]P. F. Hinrichsen and C. P. Swann, Phys. Rev. 140, B549 (1965).
[29]J. H. Hough. Z. B. duToit, and W. L. Mouton, Nucl. Phys. A109, 393 (1968).
[30]L. E. Cannell (private communication).
[31]R. M. Laszewski and P. Axel, Phys. Rev. C 19, 342 (1979).
[32]C. P. Swann, Phys. Rev. Lett. 32, 1449 (1974).
[33]F. C. Young, A. S. Figuera, and G. Pfeufer, Nucl. Instrum. Methods 92, 71 (1971).
[34]M. B. Lewis, Nucl. Data Sheets B5, 243 (1971).
[35]K. Ackermann, Diploma thesis, University of Giessen,

1978 (unpublished).
[36]C. P. Swann, J. Franklin Inst. 298, 321 (1974).
[37]C. P. Swann, Nucl. Phys. A201, 534 (1973).
[38]D. F. Coope, John M. Hanly, S. N. Tripathi, and M. T. McEllistrem, Phys. Rev. C 19, 1179 (1979).
[39]K. Reibel and A. K. Mann, Phys. Rev. 118, 701 (1960).
[40]E. G. Fuller and Evans Hayward, Nucl. Phys. 33, 431 (1962).
[41]P. Axel, K. Min, N. Stein, and D. C. Sutton, Phys. Rev. Lett. 10, 299 (1963).
[42]J. W. Knowles, A. M. Khan, and W. F. Mills, Can. J. Phys. 56, 1021 (1978).
[43]R. Moreh, S. Shlomo, and A. Wolf, Phys. Rev. C 2, 1144 (1970).
[44]Taun Ran Yeh and H. Lancman, Phys. Rev. C 16, 1268 (1977).
[45]W. Scholz, H. Bakhru, R. Colle, and Angela Li-Scholz, Phys. Rev. C 9, 1568 (1974).
[46]R. J. Sparks, H. Lancman, and C. Van der Leun, Nucl. Phys. A259, 13 (1976).
[47]R. M. Laszewski, Ph.D. thesis, University of Illinois, 1975 (unpublished).
[48]F. Ajzenberg-Selove, Nucl. Phys. A281, 1 (1977).
[49]A. Richter, in Proceedings of the International Conference on Nuclear Physics with Electromagnetic Interactions, Mainz, 1979 (unpublished); W. Knüpfer, R. Frey, A. Friebel, W. Mettner, D. Meuer, A. Richter, E. Spamer, and O. Titze, Phys. Lett. 77B, 367 (1978).
[50]J. G. Cramer, P. von Brentano, G. W. Phillips, H. Ejiri, S. M. Ferguson, and W. J. Braithwaite, Phys. Rev. Lett. 21, 297 (1968).
[51]C. P. Swann, Phys. Rev. C 16, 2426 (1977).
[52]E. D. Earle, A. J. Ferguson, G. van Middlekoop, G. A. Bartholomew, and I. Berqvist, Phys. Lett. 32B, 471 (1970).
[53]S. J. Freedman, C. A. Gagliardi, G. T. Garvey, M. A. Oothoudt, and B. Svetitsky, Phys. Rev. Lett. 37, 1606 (1976).
[54]A. M. Nathan, R. Starr, R. M. Laszewski, and P. Axel, Phys. Rev. Lett. 42, 221 (1979).
[55]D. J. Horen, R. T. Kouzes, D. Mueller, F. Calaprice, and R. P. Hall, Phys. Rev. C 19, 549 (1979).
[56]S. Raman, R. S. Hicks, R. A. Lindgren, B. Parker, and G. A. Peterson, Bull. Am. Phys. Soc. 24, 845 (1979).
[57]S. Raman, *Neutron Capture Gamma-Ray Spectroscopy*, edited by Robert E. Chrien and Walter R. Kane (Plenum, New York, 1979), p. 193; R. J. Holt, H. E. Jackson, R. M. Laszewski, and J. R. Specht, Phys. Rev. C 20, 93 (1979).
[58]C. F. Moore, J. G. Kulleck, P. von Brentano, and F. Rickey, Phys. Rev. 164, 1559 (1967).
[59]D. A. Bromley and J. Weneser, Comments Nucl. Part. Phys. 2, 151 (1968).
[60]R. Ballini, N. Cindro, J. Delaunay, J. P. Fouan, O. Nathan, and J. P. Passerieux, Phys. Lett. 26B, 215 (1968).
[61]M. Dost and W. R. Hering, Phys. Lett. 26B, 443 (1968).
[62]G. E. Brown and M. Bolsterli, Phys. Rev. Lett. 3, 472 (1959); G. E. Brown, *Unified Theory of Nuclear Models and Forces* (North-Holland, Amsterdam, 1971).
[63]M. Mizumoto, S. Raman, R. L. Macklin, G. G. Slaughter, J. A. Harvey, and J. H. Hamilton, Phys. Rev. C 19, 335 (1979); D. J. Horen, J. A. Harvey, and N. W. Hill, *ibid.* 20, 478 (1979).
[64]M. R. Schmorak, Nucl. Data Sheets 22, 487 (1977).
[65]A. Wolf, R. Moreh, A. Nof, O. Shahal, and J. Tenenbaum, Phys. Rev. C 6, 2276 (1972).
[66]F. E. Bertrand and M. B. Lewis, Nucl. Phys. A168, 259 (1971).
[67]T. P. Cleary, W. D. Callender, N. Stein, C. H. King, D. A. Bromley, J. P. Coffin, and A. Gallmann, Phys. Rev. Lett. 28, 699 (1972).
[68]Nelson Stein, C. A. Whitten, Jr., and D. A. Bromley, Phys. Rev. Lett. 20, 113 (1968).
[69]Kamal K. Seth, Nucl. Data Sheets 7, 161 (1972).
[70]P. Axel, K. K. Min, and D. C. Sutton, Phys. Rev. C 2, 689 (1970).
[71]T. Chapuran, R. Vodhanel, and M. K. Brussel, Bull. Am. Phys. Soc. 22, 1022 (1977).